Faculdade de Engenharia da Universidade do Porto
Mestrado Integrado em Bioengenharia

Biomechanical Study of the Uterus during Vaginal Delivery

by

Paulo Alexandre Gomes Gonçalves da Rocha

Supervisor:
Marco Paulo Lages Parente
Auxiliary Professor, Faculty of Engineering, University of Porto

Co-Supervisor:
Renato Manuel Natal Jorge
Associate Professor, Faculty of Engineering, University of Porto

June 2013

Abstract

The biomechanical aspects of the uterus during labour are not completely understood and these informations could improve the existing childbirth simulators, in order to also improve the obstetrician training. With the extremely difficulty of *in vivo* measurements of the uterine biomechanical changes during delivery, due to clinical, technical and ethical reasons, this work presents a biomechanical simulation of the second stage of labour, in order to evaluate these changes. The purpose of this simulation is to estimate the foetal movement during delivery, due to the uterine contractions, as well as the stresses, strains and stretches induced on the uterine tissue.

Therefore, numerical simulations based on the Finite Element Method were performed. The goal of this work is to simulate the movements of the foetus and the biomechanical effects of its passage through the birth canal. The first step of this work was to adjust the constitutive model used for the uterus. Thus, a traction test simulation of a sample modelled with the constitutive model was performed, in order to achieve a good concordance with the experimental data. Then, a preliminary work was executed, a simplified birth simulation, in order to assure if the uterine contractions were correctly simulated. Finally, two types of realistic birth simulations were performed: the extension cardinal movement of the second stage of labour with and without imposed foetal trajectory. In both simulations, the foetus was in the vertex presentation and in the occipito-anterior position. The geometrical model of the uterus, including the uterine fibres orientation, used in the realistic birth simulations was entirely designed during this work.

Keywords: Uterus, biomechanics, labour, numerical simulations, finite element method.

Contents

List of Figures

Chapter 1

Introduction

1.1 Introduction

Childbirth is an event whose biomechanical aspects are not completely understood, specially regarding the uterus. Thus, this work has the goal of deepen the current knowledge, by studying the mechanical aspects, such as tensions, deformations and contact pressures, regarding the human uterus during vaginal delivery. This knowledge can help the development of childbirth simulators.

The medical training regarding childbirth for new obstetricians involves, normally, performing real deliveries under supervision. This procedure becomes more complex when the use of deliver-helping instruments, forceps or suction cups, is required. A survey [Dupuis et al., 2003] showed that out of 4.589 births, approximately 150 resulted in lesions to the foetus. Additionally, the number of Caesarean sections reached the 20%, nearly doubling in the last 20 years. This increase may be due to the fact that the new obstetricians do not dare to perform these more complex deliveries. Thus, teaching with childbirth simulation tools would be an improvement to the actual teaching method, as almost 90% of the obstetricians who answered the survey approved. Thus, rendering the new doctors capable of performing the more complicated deliveries would reduce the number of Caesarean sections, decreasing the costs of the childbirth and the post-delivery complications.

Currently many physical interface simulators exist, which make medical training for instrumented delivery possible. Their interface is normally composed by several physical parts, representing the anatomic parts and a motorized articulated system that drives these parts, simulating the interaction of the foetus with the organs of the parturient woman and the obstetrician. Thus, these haptic simulators enable the obstetrician to increase his experience, due to the similarities between the anatomical representation given by plastic parts and reality.

However these haptic tools are not completely realistic and it would be inter-

esting to improve them, making it possible to take into consideration the various anatomical and morphological structures of the foetus and the parturient woman. These simulators use Virtual Reality techniques and are composed by two parts: a computational model that simulates the birth process and a haptic interface. The implementation of the computerized simulation part could take place through the definition of a complete three-dimensional anatomical representation of the maternal pelvis and the foetus.

Our aim is to help in the process of developing the most realistic birth simulator possible. In order to achieve that, we will focus on the computational models and simulations.

Thus, two different simulations will be performed: vaginal delivery with and without foetal imposed trajectory. In the second case, the foetus will be driven solely by the uterine contractions and the maternal pushing. Both simulations will give knowledge about the mechanical aspects of the uterus and the results of the foetal movements in the simulation without imposed trajectory could be included in a haptic simulator.

The Finite Element Method (FEM) has been chosen as the numerical resolution technique to validate our approach due to its stability and precision.

Chapter 2

Literature Review

This chapter was based on the works of Standring [Standring et al., 2008] and Hall [Hall, 2010].

2.1 Uterus

2.1.1 Introduction

The uterus is an inverted pear-shaped organ of the female reproductive system of most mammals, including humans. It is hollow, with thick muscular walls. These walls are the principal responsible for the foetal expulsion during vaginal delivery, through a set of uterine contractions that are variable in time, intensity, duration and frequency [Maul et al., 2003; Bastos et al., 2012]. During gestation, the uterus undergoes through great changes, since it is the receptacle were the foetus is developed during the entire gestation period. Thus, its walls need to adapt, stretching and distending themselves, to bear the foetus growth, while continually supplying all the foetal needs for its natural growing. The foetus normally develops completely in the uterus, in placental mammals like humans.

The uterus is supplied by arterial blood both from the uterine artery and the ovarian artery. The nerves present in the uterus are derived from the hypogastric and ovarian plexuses, and from the third and fourth sacral nerves.

2.1.2 Location

The normal, non-pregnant, uterus is usually located in the lesser pelvis, with its body lying on the urinary bladder, while its cervix lies between the urinary bladder and the rectum. The uterus is approximately 7.5 cm long, 5 cm wide, and 2 cm thick and weighs approximately 90g, despite possible and considerable size variations,

in non-pregnant woman. Its size during pregnancy can vary significantly in each woman and each pregnancy.

2.1.3 Anatomy

The uterus is divisible into two main parts: corpus and cervix.

The corpus, or body, of the uterus comprehends its superior two thirds and lies between the layers of the broad ligament, being freely movable. It has two surfaces: vesical (related to the bladder) and intestinal. It is composed mainly by muscular tissue.

The cervix is the cylindrical, narrow inferior third portion of the uterus, where it joins with the superior end of the vagina through the external orifice, or external os, which is surrounded in turn by a narrow space, the vaginal fornix. The cervix measures approximately 2.5 cm in an adult non-pregnant woman. It is mostly fibrous and is composed mainly of collagen with a small amount of smooth muscle and elastin. The amount of muscular tissue in the cervix is markedly less than in the body of the uterus. The corpus is demarcated from the cervix by the internal orifice, also known as internal os, of the uterus. It corresponds to a slight constricted segment, approximately 1 cm long, known as the isthmus of the uterus. The fundus is the rounded superior part that lies superior to the orifices of the Fallopian tubes, also called uterine tubes.

All the anatomical elements of the uterus are represented on Figure 2.1.

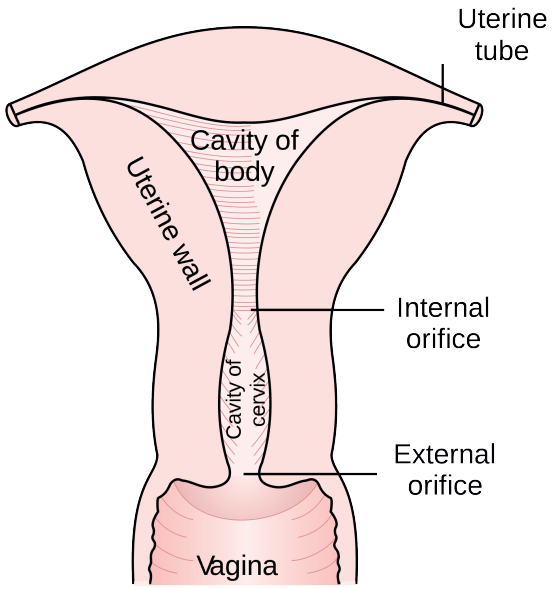

Figure 2.1: Uterus and uterine tubes representation. From [Standring et al., 2008].

The uterus' walls are constituted by three layers. From the outermost to the innermost, there are: perimetrium, myometrium and endometrium.

2.1.3.1 Perimetrium

The perimetrium consists of peritoneum, supported by a thin layer of connective tissue. It is the serosa or outer serous layer, and extends laterally into the broad ligament.

2.1.3.2 Myometrium

The myometrium is the middle muscular layer, consisted by smooth muscle. The main blood vessels and nerves of the uterus are located in this layer. It is constituted by three layers, whose muscle fibres' orientation is represented on Fig. 2.2. These muscle fibres contract during childbirth and are the responsible for the expulsion of the foetus. During pregnancy, the thickness of this layer varies at several points of the uterus, but it has an average thickness of approximately 9mm [Degani et al., 1998].

2.1.3.3 Endometrium

The endometrium is the inner mucous layer and is firmly adhered to the underlying myometrium. During the menstrual cycle, it undergoes severe structural changes at each stage of the cycle: the endometrium periodically builds a lining, called decidua, to receive the ovum, i.e. the implantation. This implantation leads to pregnancy. This lining is shed if no ovum is implanted into the uterus, as can be seen on Fig. 2.3. This shedding of the endometrium is the cause for the menstrual bleeding.

2.1.4 Menstrual Cycle

The menstrual cycle is the group of physiological changes that occur in fertile women with the objective of sexual reproduction. A normal cycle lasts 28 days. During this cycle, the uterus goes through three phases: proliferative, secretory and menstrual.

2.1.4.1 Proliferative

In the early proliferative phase, even before the menstrual flow ceases, the epithelium from the persisting basal parts of the uterine glands grows over the surface of the endometrium which has been denuded by menstruation. Re-epithelialization is complete 5—6 days after the start of menstruation. Initially, the tissue is only 1—2 mm thick. During days 10—12 of the proliferative phase, the endometrium

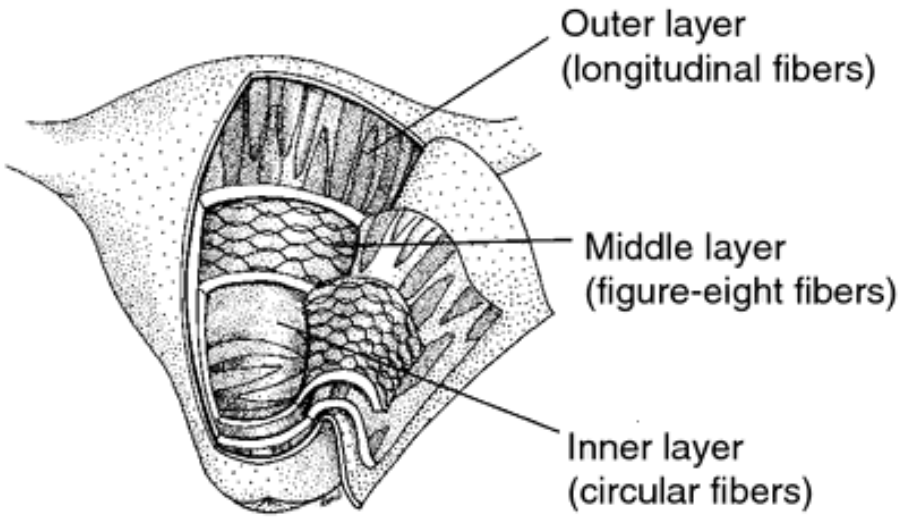

Figure 2.2: Orientation of the fibres of the three layers of the myometrium. From [Murray et al., 2006].

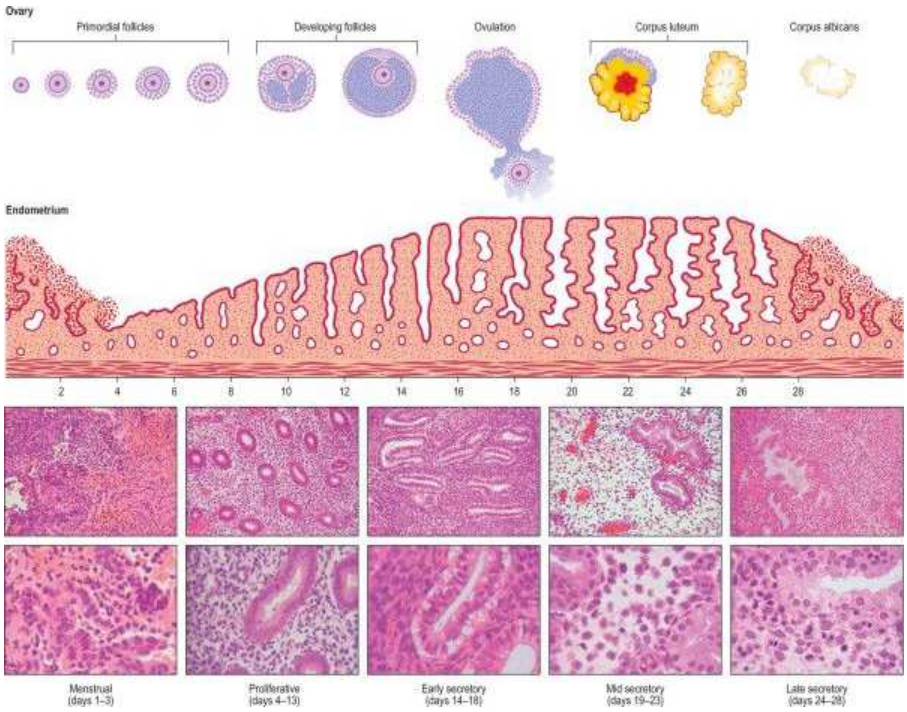

Figure 2.3: The menstrual cycle. From [Standring et al., 2008].

thickens. Cells divide in response to rising levels of oestrogen which is produced by the ovaries.

2.1.4.2 Secretory

The secretory phase coincides with the luteal phase of the ovarian cycle. The endometrial changes are driven by progesterone and oestrogen secreted by the corpus luteum. In the following 7 days, the endometrium activates a sequence of differentiative events, required to prepare the tissue for blastocyst implantation. The first morphological effects of progesterone are evident 24—36 hours after ovulation (which occurs 14 days before the next menstrual flow). By the mid-secretory phase the endometrium may be up to 6 mm deep. There is evidence for collagen synthesis and degradation, presumably reflecting ongoing matrix remodelling. In the late secretory phase, glandular secretory activity declines. Decidual differentiation occurs in the superficial stromal cells that surround blood vessels.

2.1.4.3 Menstrual

As regression of the corpus luteum occurs, those parts of the stroma showing a decidual reaction undergo degenerative changes and the endometrium often diminishes in thickness. Blood escapes from the superficial vessels of the endometrium forming small haematoma beneath the surface epithelium. 65 — 75% of the thickness of the endometrium may be shed. Blood and necrotic endometrium then begin to appear in the uterine lumen, to be discharged from the uterus through the vagina as the menstrual flow, which lasts from 3 to 6 days.

2.1.5 Changes during Pregnancy

During pregnancy, many morphological changes occur in the female reproductive system and associated abdominal structures. The uterus enlarges to accommodate the developing foetus and placenta, and various alterations take place in the pelvic walls, floor and contents which allow for this expansion, and which anticipate parturition. At the end of gestation, dramatic changes occur that facilitate the passage of the baby through the birth canal.

The function of the uterus in pregnancy is to retain the developing foetus and to provide a protected environment until a stage, at which the foetus is capable of surviving *ex utero*. In order to achieve this, the uterus must grow with the development of the foetus. Thus, smooth muscle cells must be stretched without leading to miscarriage or premature labour.

The uterus grows dramatically during pregnancy, increasing in weight from about 50 g at the beginning of pregnancy to up to 1 kg at term. Most of the weight

gain is the result of increased vascularity and fluid retention in the myometrium. The increased growth of the uterine wall is driven by a combination of mechanical stretching and endocrine input. The mechanical load that the growing foetus imposes on the uterine wall induces hypertrophy of uterine smooth muscle cells, and is the major stimulus that increases smooth muscle mass. Some hyperplasia, cell proliferation, occurs early on in pregnancy, mainly from the growth of the media of the myometrial arteries and veins. The myometrium thins with advancing gestation, from 20—30 mm thick in early pregnancy to 10—20 mm at term.

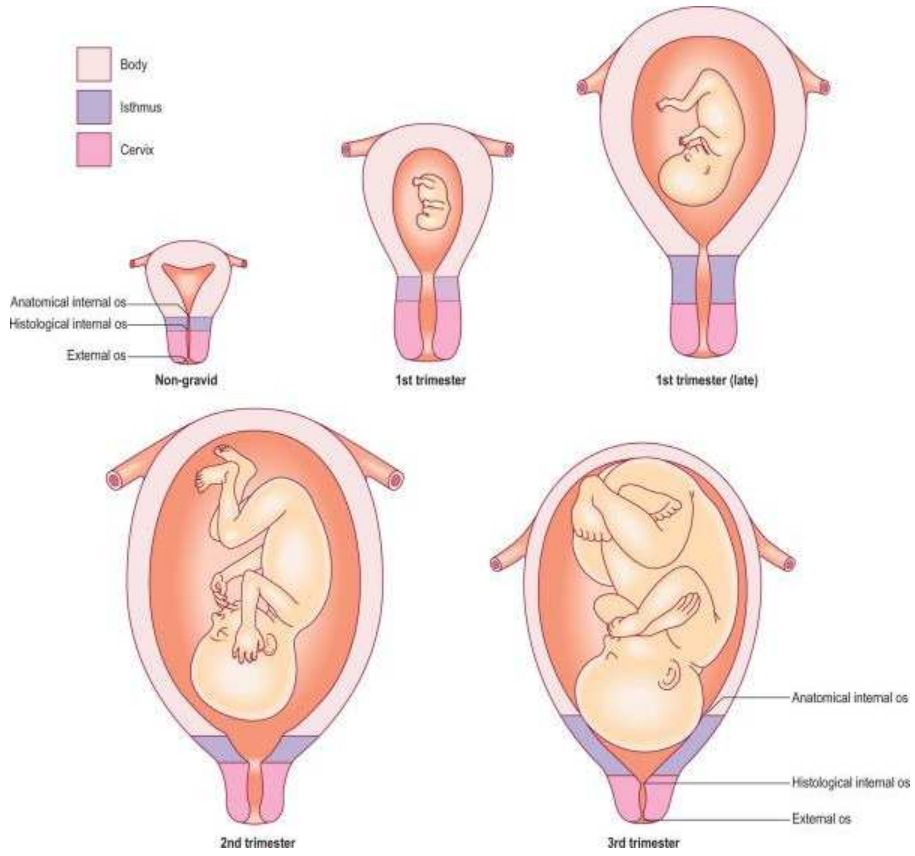

Figure 2.4: Frontal view of the uterus showing the location and extent of the body, isthmus and cervix in the non-gravid and gravid uterus at different stages in gestation. The isthmus forms the lower uterine segment with advancing gestation. From [Standring et al., 2008].

The isthmus is gradually taken up into the uterine body during the second month to form the "lower segment", as seen on Fig 2.4. The isthmus hypertrophies like the uterine body during the first trimester and triples in length to about 3 cm.

The cervix is required to serve two functions in relation to pregnancy and par-

turition. During pregnancy, it is a relatively rigid fibromuscular structure which retains the developing foetus within the uterus. During active labour the cervix dilates to allow the foetus to descend through the birth canal. Considerable softening and shortening of the cervix occurs in the weeks before the onset of labour; a corresponding increase in uterine activity is usually apparent during this pre-labour period. The rigidity of the cervix appears to be related to the orientation of its collagen fibres within a regular connective tissue matrix. The exact processes that allow softening, effacement and dilatation of the cervix are unclear, but are believed to include remodelling of the connective tissue matrix.

2.1.6 Physiology

2.1.6.1 Pregnancy

Before pregnancy, the uterus undergoes several structural changes, due to the menstrual cycle. This cycle causes the uterus to be prepared for the arrival of one or more ova. If the fecundation occurs, the zygote, fecundated ovum, will be implanted into the uterus, where it develops into the foetus and placenta. This can only occur in a certain time-frame of the menstrual cycle. If the menstrual phase is not the appropriate or the ovum is not fertilized, implantation does not occur, as so the pregnancy.

2.1.6.2 Labour

During labour, the function of the uterus is to expel the foetus to the exterior. This is achieved by the uterine contractions, that push the foetus downward. These contractions are hormonally stimulated, by the oxytocin hormone, and occur at intervals of decreasing length to dilate the external orifice and expel the foetus and placenta.

2.2 Pelvic Floor

The pelvic floor is composed of muscle fibres of the levator ani, the coccygeus, and associated connective tissue which span the area underneath the pelvis. It separates the pelvic cavity above from the perineal region (including perineum) below and is important in providing support for pelvic viscera (bladder, intestines, the uterus—in females) and in maintenance of continence as part of the urinary and anal sphincters.

Regarding the childbirth, the pelvic floor facilitates birth by resisting the descent of the presenting part of the foetus, causing it to rotate forwards to navigate through the pelvic girdle.

2.3 Labour

Childbirth, or labour, is the last step of the human gestation period, also called pregnancy, and is characterized by the expulsion of one or more foetuses from the woman's uterus. A typical childbirth, by vaginal delivery, can be divided in 3 stages.

2.3.1 First Stage of Labour

The first state of labour begins with the start of uterine contractions that cause progressive changes in the cervix and ends when the cervix is fully dilated. This stage is divided into two phases: latent and active labour, whose last part is known as transition. This stage is the longest one.

During early labour, the cervix gradually effaces and dilates. Early labour starts once the contractions are occurring regularly, 10 minutes apart and lasting 30 seconds, and the cervix begins to progressively dilate and efface. During this phase, the contractions become longer and stronger until being separated by 5 minutes and lasting 40—60 seconds. This phase usually ends when the cervix is about 3—4 centimetres dilated and the labour progress accelerates.

Following early labour, active labour starts. This phase occurs when the contractions are occurring every 3—5 minutes and lasting 40—60 seconds. With active labour, the cervix begins to dilate more rapidly and the contractions are longer, stronger and closer in time. During this stage, the cervix dilates from about 3—4 centimetres to 10 centimetres. The baby generally starts to descend during this phase.

This transition occurs when the cervix dilates from 8—10 centimetres. It is called transition because it marks the shift into the second stage of labour. This time frame is when the most intense part of labour occurs. Contractions are usually very strong, occurring every 2—3 minutes and lasting a minute or more. The transition period may take anywhere from a few minutes to a few hours. By the time the cervix is fully dilated and the transition is over, the baby has usually descended somewhat into the pelvis.

2.3.2 Second Stage of Labour

The second stage of labour begins once the cervix is fully dilated and ends with the expulsion of the foetus. At the beginning of this stage, the contractions may be a little further apart. When the uterus contracts it puts pressure on the foetus. That pressure, along with the pushing done by the woman, will move the foetus into the birth canal. This movement may be rapid or gradual. When a contraction is over and the uterus relaxes, the babies head will recede slightly. When the widest part of the foetus' head is finally visible, it is crowning. Shortly after the crowning, the

foetus' face will begin to appear and the woman will then be encouraged to continue pushing so that the shoulders and body can be delivered.

The entire second stage can last anywhere from a few minutes to several hours.

2.3.3 Third Stage of Labour

The third stage of labour begins after the birth of the foetus and ends with the separation and subsequent delivery of the placenta. Minutes after giving birth, the uterus will contract again. The first several contractions usually separate the placenta from the uterine wall, and it is expelled with the help of some pushes. This process usually takes 5—10 minutes.

2.4 Mechanics of the Labour

The uterine contractions during labour begin at the fundus and spread downward over the corpus. Thus, the intensity of the contraction is greater at the top of the corpus and it decreases to the cervix. Therefore, each uterine contraction forces the baby to descend toward the cervix.

The combined contractions of the uterine and abdominal musculature during delivery cause a downward force on the foetus of about 25 pounds (approximately 11 kilograms) during each contraction. Intrauterine pressure during the second stage of labour can arise to 0.4 MPa [Buhimschi et al., 2004].

The uterine contractions are intermittent because strong ones impede or sometimes even stop blood flow through the placenta. If the contractions were continuous, it could cause the death of the foetus. Indeed, overuse of various uterine stimulants, such as oxytocin, can cause uterine spasm rather than rhythmical contractions and can lead to the death of the foetus.

2.4.1 Cardinal Movements

The cardinal movements refer to the position changes of the foetal head during its passage through the birth canal, in a labour in the vertex position. Despite being a continuous process, delivery can be divided in seven discrete cardinal movements: engagement, descent, flexion, internal rotation, extension, external rotation, and expulsion (Figure 2.6).

Engagement Engagement refers to passage of the widest diameter of the presenting part by the plane of the pelvic inlet (Fig. 2.5).

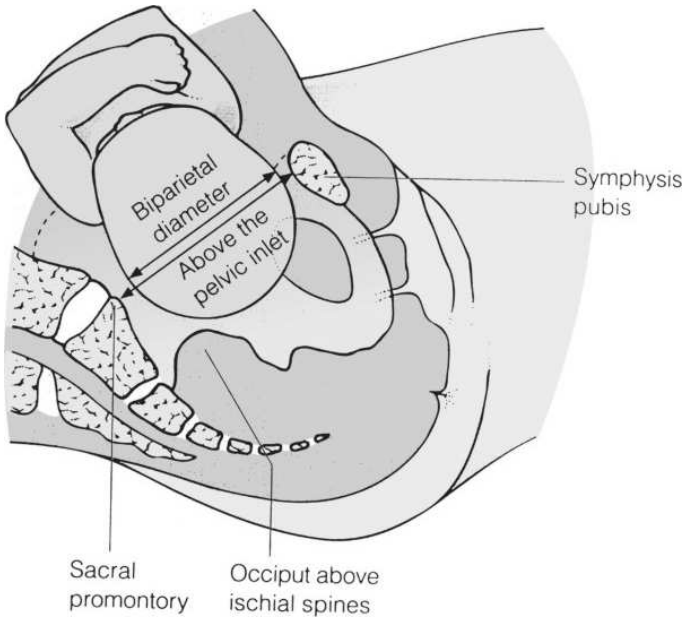

Figure 2.5: Engagement of the foetal head. Adapted from [Gabbe et al., 2007].

Descent Descent refers to the downward passage of the presenting part through the pelvis.

Flexion Flexion of the foetal head occurs passively, due to the shape of the bony pelvis, as the head descends. The result of complete flexion is to present the smallest diameter of the foetal head (the suboccipitobregmatic diameter) for the passage through the pelvis.

Internal Rotation Internal rotation refers to rotation of the presenting part from its original position as it enters the pelvic inlet to the anteroposterior position as it descends through the pelvis, rotating the occiput of the foetus towards the pubic symphysis. This allows the widest portion of the foetus to face the pelvis at its widest dimension. As well as flexion, internal rotation is a passive movement resulting from the shape of the pelvis and the pelvic floor musculature.

Extension Because the vaginal outlet is directed upward and forward, extension of the foetal head must occur before the head can pass through it. As the head continues its descent, crowning, when the largest diameter of the foetal head is encircled by the vulvar ring, occurs.

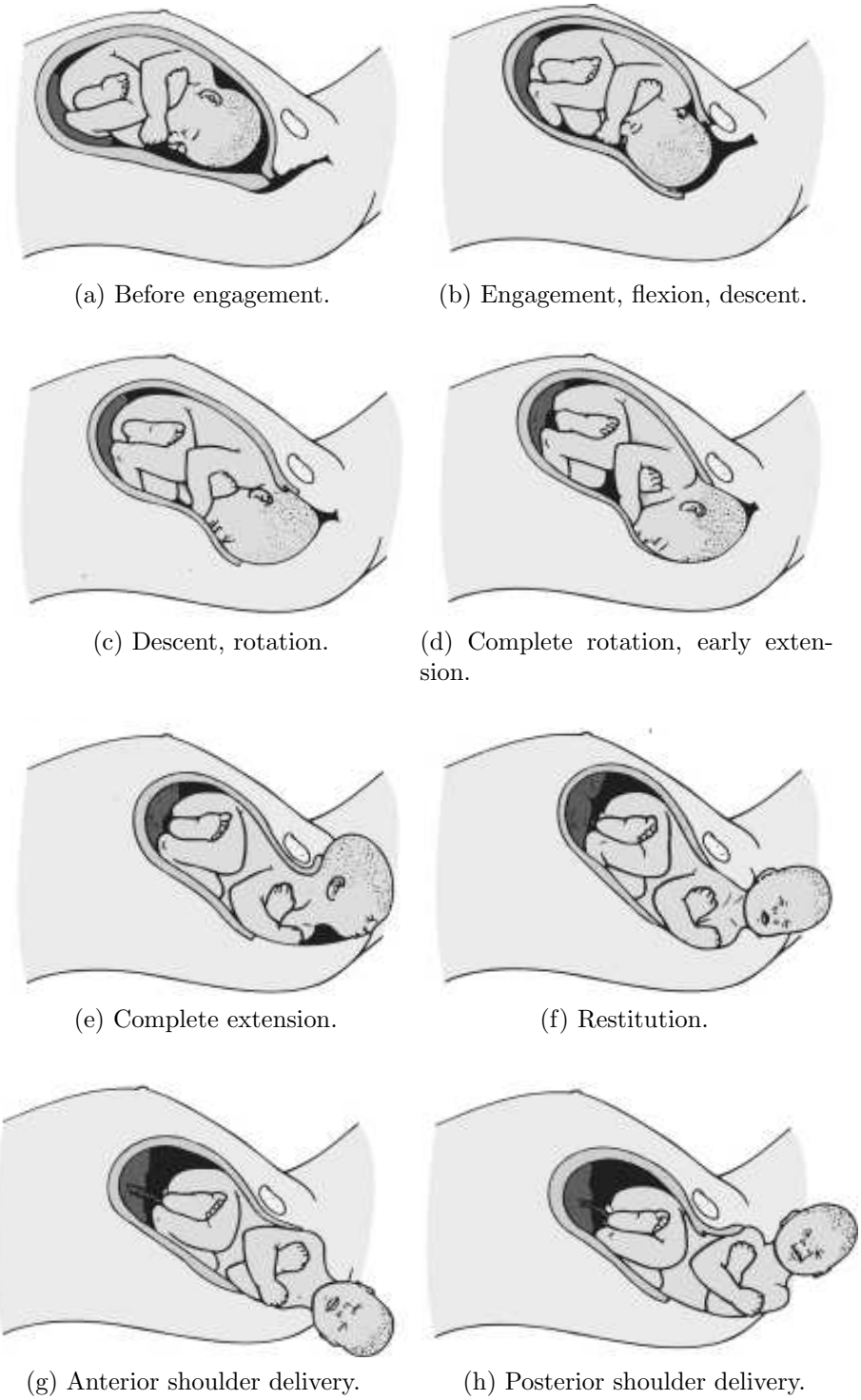

(a) Before engagement.

(b) Engagement, flexion, descent.

(c) Descent, rotation.

(d) Complete rotation, early extension.

(e) Complete extension.

(f) Restitution.

(g) Anterior shoulder delivery.

(h) Posterior shoulder delivery.

Figure 2.6: Cardinal movements during labour. Adapted from [Gabbe et al., 2007].

External Rotation External rotation, also known as restitution, follows delivery of the head when it rotates to the position it occupied at engagement. Following this, the shoulders descend in a path similar to that traced by the head.

Expulsion Expulsion refers to delivery of the rest of the foetus. After delivery of the head and external rotation, further descent brings the anterior shoulder to the level of the pubic symphysis . The anterior shoulder is delivered in much the same manner as the head, with rotation of the shoulder under the pubic symphysis. After this, the rest of the body is normally delivered without difficulty.

2.4.2 Influence of the Foetus

The foetus itself has a great influence in the course of the labour [Gabbe et al., 2007]. Some of the variables are listed and explained below. Abnormalities in the these foetal variables may affect greatly the course of and the likelihood of vaginal delivery.

Fetal size The foetus size can be estimated clinically by abdominal palpation or with ultrasound, but both are subject to a large degree of error. Foetal macrosomia, a foetus with excessive weight, is associated with an increased likelihood of failed labour [Spellacy et al., 1985].

Lie Lie is called to the position of the longitudinal axis of the foetus relative to the longitudinal axis of the uterus. Foetal lie can be either longitudinal, transverse, or oblique (Figure 2.7).

Presentation Presentation of the foetus refers to the foetal part that directly overlies the pelvic inlet. In a foetus presenting in the longitudinal lie, the presentation can be cephalic (vertex) or breech. In a cephalic foetus, which occurs in 95% of the cases, the presentation is classified according to the leading bony landmark of the skull, which can be either the occiput (vertex), the chin (mentum), or the brow (Figure 2.8).

Attitude Attitude refers to the position of the head with regard to the foetal spine, i.e. the degree of flexion or extension of the foetal head. Flexion of the head is important to facilitate engagement of the head in the maternal pelvis. When the foetal chin is flexed onto the chest, the smallest possible diameter of the head is presented at the pelvic inlet (suboccipitobregmatic diameter, 9.5 cm, Fig. 2.9. As the extension of the head occurs, the diameter presenting to the pelvic inlet progressively

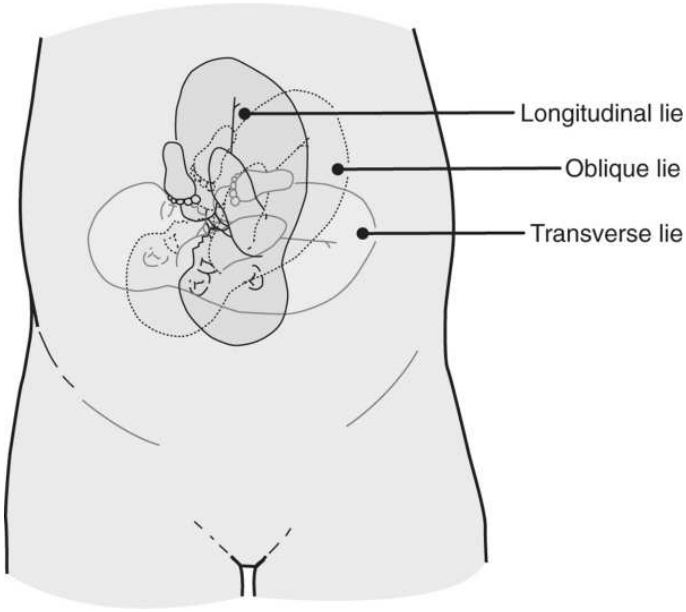

Figure 2.7: Examples of different fetal lie. Adapted from [Gabbe et al., 2007].

increases. The architecture of the pelvic girdle bones along with increased uterine activity help positioning the foetal head in the correct flexion for labour.

Position Position of the foetus refers to the relationship of the foetal presenting part to the maternal pelvis. For cephalic presentations, the fetal occiput is the reference. If the occiput is directly anterior, the position is occiput anterior. If the occiput is turned toward the mother's right side, the position is right occiput anterior. The various positions of a cephalic presentation are illustrated in Figure 2.10. Most commonly, the foetal head enters the pelvis in a transverse position and, then as a normal part of labour, rotates to an occiput anterior position.

2.5 Numerical Simulations

The simulation techniques, using mathematical methods, have been created and improved along with the computational systems' development, in order to substitute the real mechanical assays. The aim of these numerical methods is to design and analyse the approximate but accurate solutions for hard problems.

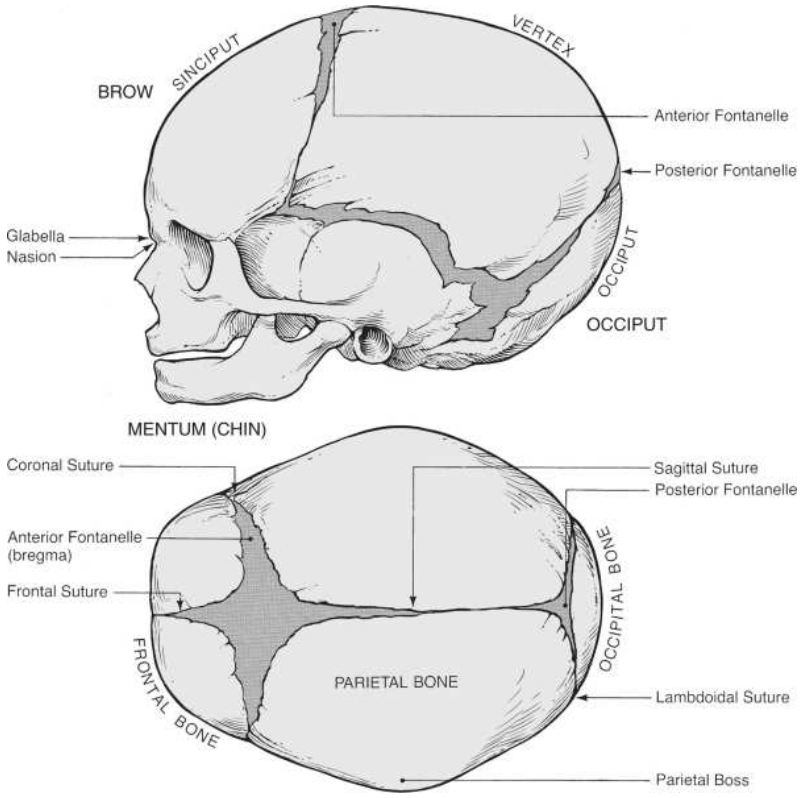

Figure 2.8: Landmarks of foetal skull for determination of foetal position. Adapted from [Gabbe et al., 2007].

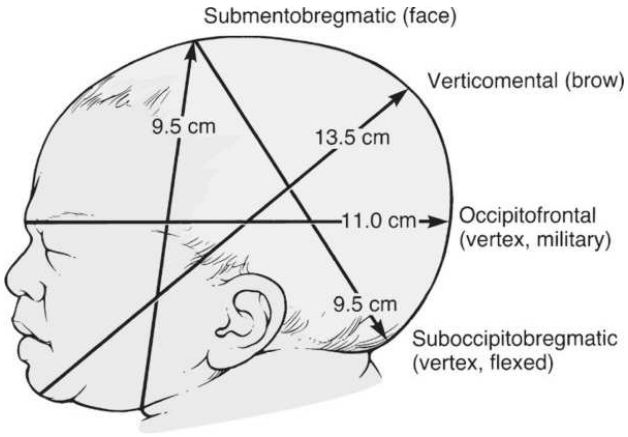

Figure 2.9: Presenting diameters of the average term foetal skull. Adapted from [Gabbe et al., 2007].

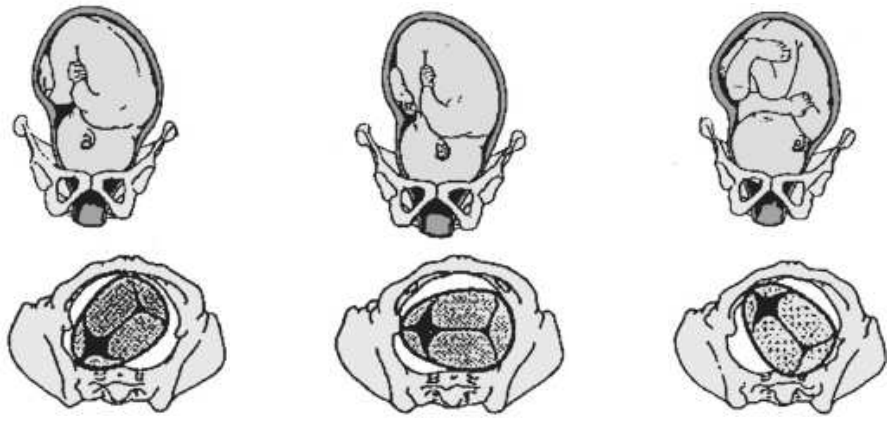

(a) Left occiput anterior.

(b) Left occiput transverse.

(c) Left occiput posterior.

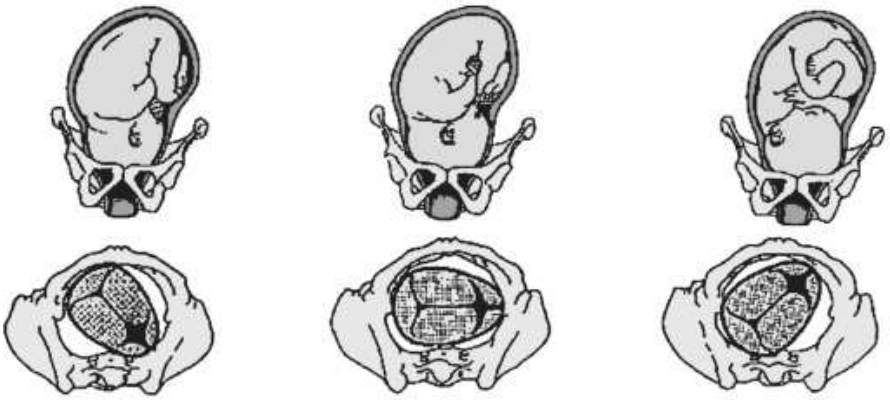

(d) Right occiput anterior.

(e) Right occiput transverse.

(f) right occiput posterior.

Figure 2.10: Foetal presentations and positions in labour. From ([Gabbe et al., 2007]).

2.5.1 Finite Element Method

The most world-wide used numerical method is the Finite Element Method (FEM), which was developed in the 1940's and nowadays is a tool used in a huge variety of fields, such as civil engineering, electromagnetic working environments, biomechanics or aeronautics, solving a variety of practical engineering problems. As its underlying theory is well established, it is recognized as one of the most powerful numerical analysis tool to analyse complex problems of engineering.

The FEM is a computer-aided mathematical technique for obtaining approximate numerical solutions to the equations of calculus that predict the response of physical systems subjected to external influences. It consists of a computer model of a material or design that is stressed and analysed for specific results. It is used in product design and refinement. Thus, it is possible to verify if a proposed design will be able to perform to the specifications prior to manufacturing or construction. Modifying an existing product or structure is utilized to qualify the product or structure for a new service condition. In case of structural failure, FEM may be used to help determine the design modifications to meet the new condition.

Regarding biomechanics, FEM is used in the prosthetics field, allowing the prevision of complication that can arise. Prostheses and other medical devices are subjected to a wide range of biomechanical tests before they can be implanted in the body. These pre-clinical tests are important in order to protect the patients against ineffective devices, so they are not conducted directly on the patients. Thus, a FEM model is constructed to be used in those experiments. This method is currently being widely used in the simulation of childbirths, in order to understand better the biomechanical perspective of this remarkable event.

Chapter 3

State of the Art

3.1 Mechanical Properties

3.1.1 Uterus

In order to completely understand the biomechanical aspects of the uterus, its mechanical properties must be well known. Due to the complexity of the uterus, its different parts have different functions and, consequently, different mechanical properties. Thus, the myometrial and cervical tissues' mechanical properties and their change during gestation and labour were already deeply studied. Sheep [Parkington, 1985] and rat [Izumi, 2012] myometrial tissue was studied, such as rat cervix [Harkness and Harkness, 1959, 1961; Rahn et al., 2008] and human cervical tissue [Mazza et al., 2006; Myers et al., 2008]. Dynamical tension tests on human uterus tissues were also performed [Manoogian et al., 2012]. The volume of the human uterine cavity as a function of pressure was determined [Niederer et al., 2009], thus understanding the pressure-volume relationship.

3.1.2 Pelvic Floor

The human pelvic floor mechanical properties were already studied by Jing [Jing, 2010], which was the first work to measure its biaxial visco-hyperelastic properties. Other anterior studies used data from other soft tissues such as cardiac tissue [Aulignac et al., 2005; Martins et al., 2007; Parente et al., 2008, 2009a,b; Calvo et al., 2009], tongue and facial muscles [Lee et al., 2005] and skeletal muscles [Li et al., 2008].

3.2 Computer Models

The structural complexity of all the structure to model (uterus, foetus, pelvic floor) before and during birth brings difficulties to the finite element modelling. Thus, it is necessary to construct an anatomically correct geometrical mode and to select the appropriate constitutive models.

Some computer models of the uterus were already developed [Buttin et al., 2009; Niederer et al., 2009] and there are also several computer models of the pelvic floor function using finite element methods. Models showing levator ani muscles stretching [Lien et al., 2004], pelvic floor muscles [Aulignac et al., 2005; Lee et al., 2005, 2009; Martins et al., 2007; Li et al., 2008; Parente et al., 2008, 2009a,b], both pelvic floor and the anal canal [Noakes et al., 2006, 2008a,b], pubic symphysis [Li et al., 2006, 2007] and the vagina [Chen et al., 2009; Calvo et al., 2009].

3.2.1 Geometrical Models

3.2.1.1 Uterus

Some geometrical models of the uterus were already published, which were constructed by medical data from magnetic resonance procedures [Buttin et al., 2009; Niederer et al., 2009]. Weiss [Weiss et al., 2005] used magnetic resonance diffusion tensor imaging in order to elucidate the spatial fibre architecture within the uterine walls.

3.2.1.2 Foetus

Parente [Parente et al., 2008, 2009a,b, 2010] used anatomically correct foetal geometrical models. Lapeer [Lapeer, 1999] worked on foetal head moulding, which is an important occurrence during labour.

3.2.1.3 Pelvic Floor

Some pelvic floor models [Aulignac et al., 2005; Martins et al., 2007; Parente et al., 2008, 2009a,b] used the data from Janda [Janda et al., 2003], who used magnetic resonance imaging (MRI) and 3D-palpator measurements on a cadaver specimen. The disadvantage of these data is that they exhibit distorted spatial relations due to the complete lack of muscle tone, due to being obtained from a cadaver. Other finite element models [Lien et al., 2004; Chen et al., 2009] derived their geometrical models from *in vivo* MRI scans. Finite element meshes based on cryosection photographs from cadavers and MRI scans were also created [Noakes et al., 2006, 2008a,b]. 3-D geometries from MR scans of nulliparous females were also extracted [Lee et al.,

2005, 2009]. In addition to MRI images, CT scan data have also been used to build the geometry of the pelvic structures [Li et al., 2006, 2007].

3.2.2 Constitutive Models

A constitutive model represents the mathematical relation between two physical quantities, which is specific to a material or substance, and approximates the response of that material to external solicitations, usually as applied fields or forces. They can be combined with physical laws in order to solve physical problems. This is one of the most intensely researched field within solid mechanics because of its complexity and the importance of accurate constitutive models for practical engineering problems.

3.2.2.1 Uterus

Mizrahi et al., 1980 showed that the behaviour of the uterine muscles changed during the childbirth, with an isotropic behaviour in the early stages of childbirth and an anisotropic one with the progress of labour. Buttin [Buttin et al., 2009] has modelled the uterus as a Neo-Hookean hyperelastic material, with anisotropic behaviour. Niederer [Niederer et al., 2009] modelled the uterus, considering anisotropy, viscoelasticity and extended nonlinearity, while Weiss [Weiss et al., 2008] modelled as a viscoelastic, nonlinear, nearly incompressible and isotropic material.

3.2.2.2 Pelvic Floor

The constitutive model of the pelvic floor has several aspects that need to be considered, such as nonlinear elasticity under finite strain [Li et al., 2006, 2007, 2008; Noakes et al., 2008b; Calvo et al., 2009; Lee et al., 2005, 2009; Aulignac et al., 2005; Martins et al., 2007; Parente et al., 2008, 2009b,a], muscle fibre-induced anisotropy [Li et al., 2006, 2007; Aulignac et al., 2005; Martins et al., 2007; Parente et al., 2008, 2009a,b; Calvo et al., 2009], time-dependent behaviour [Li et al., 2006, 2007] and active muscle contraction [Aulignac et al., 2005; Martins et al., 2007; Parente et al., 2009a; Maggio et al., 2012].

3.3 Maternal-foetal Interaction

Modelling the continuously-changing maternal-foetal interaction is a highly nonlinear boundary problem due to the possibility of intermittent contact and separation. Another challenge comes from the relatively big differences of the material properties between foetal head and maternal muscles, which renders the simulation progresses much slower in order to avoid "numerical penetration". Due to these difficulties,

most of the existing pelvic floor models ignored maternal-foetal interaction, applying pressures statically on the pelvic floor[Aulignac et al., 2005; Lee et al., 2005, 2009; Noakes et al., 2008b].

Although, some pelvic floor models have begun to incorporate the maternal-foetal interaction [Martins et al., 2007; Parente et al., 2008, 2009a,b; Li et al., 2008].

3.4 Uterine Contraction Models

Uterine contractions have already been modelled [Eytan and Elad, 1999; Vauge et al., 2000; Buttin et al., 2009; Bastos et al., 2010, 2012]. Earlier studies of these contractions were presented by Taverne [Taverne et al., 1979].

3.5 Foetal Drive

Some models applied simple translational and/or rotational displacements on the foetus [Martins et al., 2007; Parente et al., 2008, 2009a,b; Li et al., 2008], while Buttin [Buttin et al., 2009] and Jing [Jing, 2010] used a more complex, dynamically time-changing pressure profile in order to drive the foetus through the birth canal. Jing [Jing, 2010] applied the pressure profile directly on the foetus, while Buttin [Buttin et al., 2009] applied it on the uterine walls.

3.6 Influence of the Foetus

The several ways in which the foetus impacts the labour have already been studied: foetal head moulding [Lapeer, 1999; Lapeer and Prager, 2001; Parente et al., 2012], foetal head flexion [Parente et al., 2010] and foetal position [Parente et al., 2009b].

Chapter 4

A constitutive model for the behaviour of the human uterine muscles

4.1 The Uterine Constitutive Model

The constitutive model adopted in this work for the active and passive behaviour of the uterine muscles is a modified form of the hyper-elastic incompressible model, transversely isotropic, suggested by Humphrey and Yin [Humphrey and Yin, 1987] and modified by Martins et al. [Martins et al., 1998] for the passive behaviour of heart muscles.

For the constitutive model used, the deformation energy function, for a quasi-incompressible material and for volume unit, in the reference configuration, may be written by:

$$U = U_I\left(\overline{I}_1^C\right) + U_J(J) + U_f(\overline{\lambda}_f, \alpha) \tag{4.1}$$

The deformation energy function (Eq. 4.1) is the result of the sum of a term related with the isotropic matrix, which soaks the muscular fibres, a second term related with the muscular fibres and a third term related with the volume variation. In Eq. 4.1, U_I is the deformation energy associated with the isotropic matrix, defined by:

$$U_I = c\left[e^{b\left(\overline{I}_1^C\right)-3} - 1\right] \tag{4.2}$$

where $\overline{I}_1^C$ is the first invariant of the Right Cauchy-Green deformation tensor, with the volume variations eliminated.

$$\overline{I}_1^C = tr\overline{\mathbf{C}} = tr\left(\overline{\mathbf{F}}^T\overline{\mathbf{F}}\right) = J^{-2/3}tr\mathbf{C} \tag{4.3}$$

with $\overline{\mathbf{F}}$ being the deformation gradient with the volume variations eliminated:

$$\overline{\mathbf{F}} = J^{-1/3}\mathbf{F} \tag{4.4}$$

and J being the volume variations:

$$J = det\,\mathbf{F} \tag{4.5}$$

In Eq. 4.1, the deformation energy stored in the different muscular fibres families is given by $\mathbf{U}_f$, which can be divided in an elastic passive component (U_{pass}) and an active component (U_{act}), due to contraction.

$$U_f\left(\overline{\lambda}_f, \alpha\right) = U_{pas}\left(\overline{\lambda}_f\right) + U_{act}\left(\overline{\lambda}_f, \alpha\right) \tag{4.6}$$

To the passive component, U_{pass}, the following expression was used:

$$U_{pas} = A\left\{exp\left[a\left(\overline{\lambda}_f - 3\right)^2\right] - 1\right\} \tag{4.7}$$

where (λ_f) represents the relation between the actual and the initial length of a muscular fibre that initially is in the $\mathbf{N}$ direction:

$$\overline{\lambda}_f = \sqrt{\mathbf{N}^T\overline{\mathbf{C}}\mathbf{N}} = \sqrt{\overline{\mathbf{C}} : (\mathbf{N}\otimes\mathbf{N})} \tag{4.8}$$

and $\otimes$ represents the tensor product. For the deformation energy due to the muscular contraction, U_{act}, the following expression was used:

$$U_{act} = \alpha T_0^M \int_1^{\overline{\lambda}_f} 1 - 4\left(\overline{\lambda}_f - 1\right)^2 \mathrm{d}\overline{\lambda} \tag{4.9}$$

where α is the activation level, varying between 0 and 1. When $0.5 < \overline{\lambda}_f < 1.5$, U_{act} is bigger than 0, and for other values of $\overline{\lambda}_f$, the muscle does not produces force, being its deformation energy null. The constant T_0^M is the maximum tension produced by the muscle for a rest state length (T_0^M=1).

In Eq. 4.1, the deformation energy associated to the volume variation is given by $\mathbf{U}_J$:

$$U_J = \frac{1}{D}(J-1)^2 \tag{4.10}$$

The parameters that resulted in a good concordance with the experimental data were the following c= 1.58×10^{-2}N/mm^2, b=1.173, A= 2.8×10^{-2}N/mm^2 and a=0.6215.

4.2 Material Tests

In order to obtain the material properties for the constitutive model used for the uterus, a numerical simulation was performed (Fig. 4.1). This simulation was a replica of the traction test performed by Manoogian [Manoogian, 2008] on human uterine tissue (Fig. 4.2). The sample's dimensions and the test's conditions were identical to the ones tested (Fig. 4.3) . The parameters that resulted in a good concordance with the experimental data were the following c= 1.58×10^{-2}N/mm^2, b=1.173, A= 2.8×10^{-2}N/mm^2 and a=0.6215, as can be seen of Fig. 4.4.

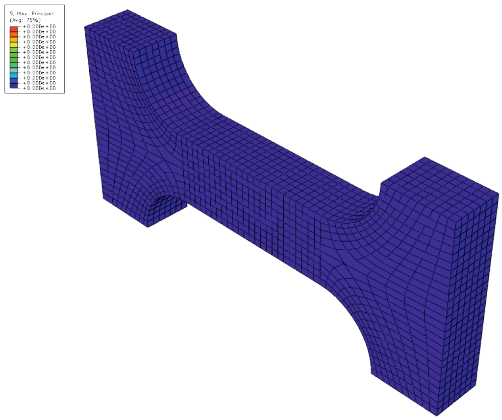

(a) The uterine sample before the traction test.

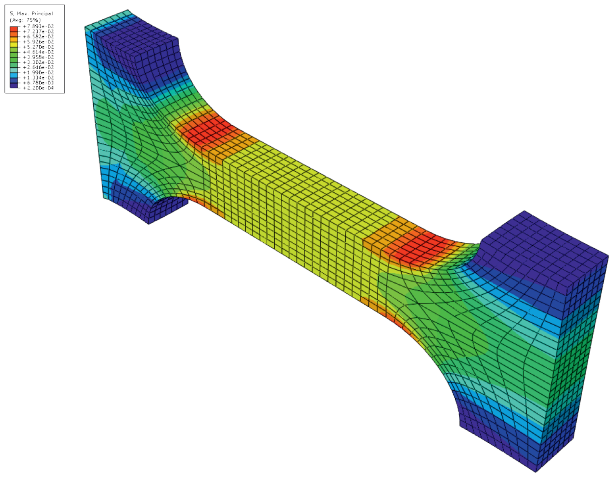

(b) The uterine sample after the traction test.

Figure 4.1: Traction test performed on a sample with the uterine material properties used.

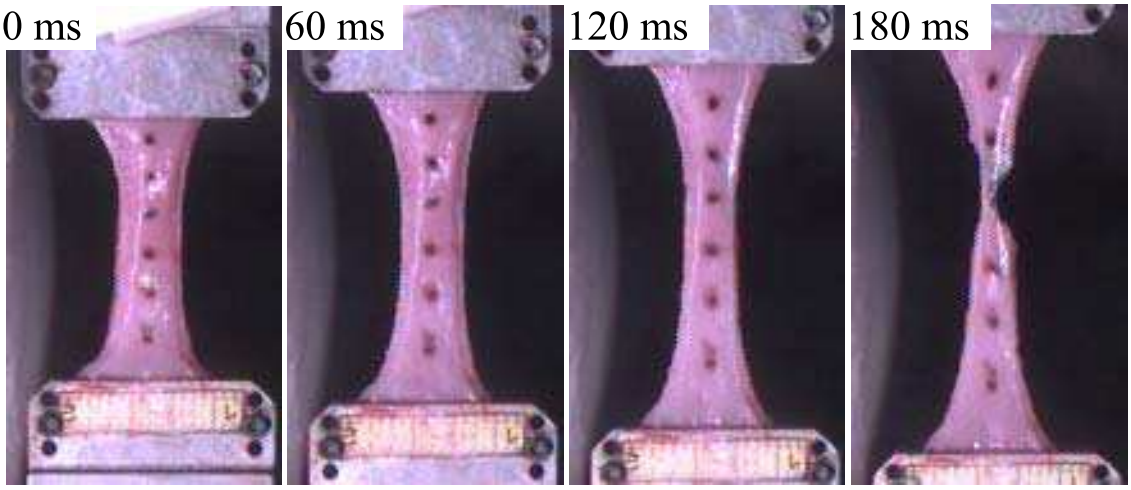

Figure 4.2: Traction test performed on uterine tissue samples, performed by Manoogian. From [Manoogian, 2008].

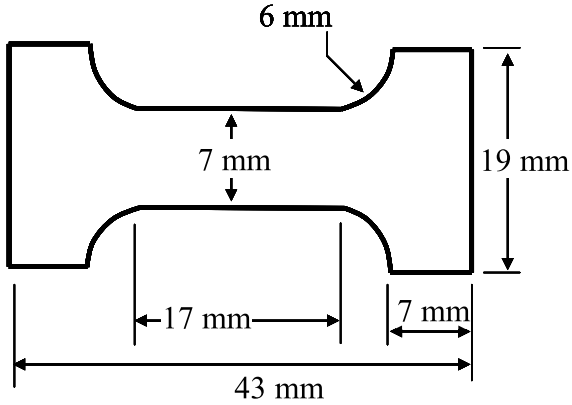

Figure 4.3: Dimensions of the sample designed to the material test. From [Manoogian, 2008].

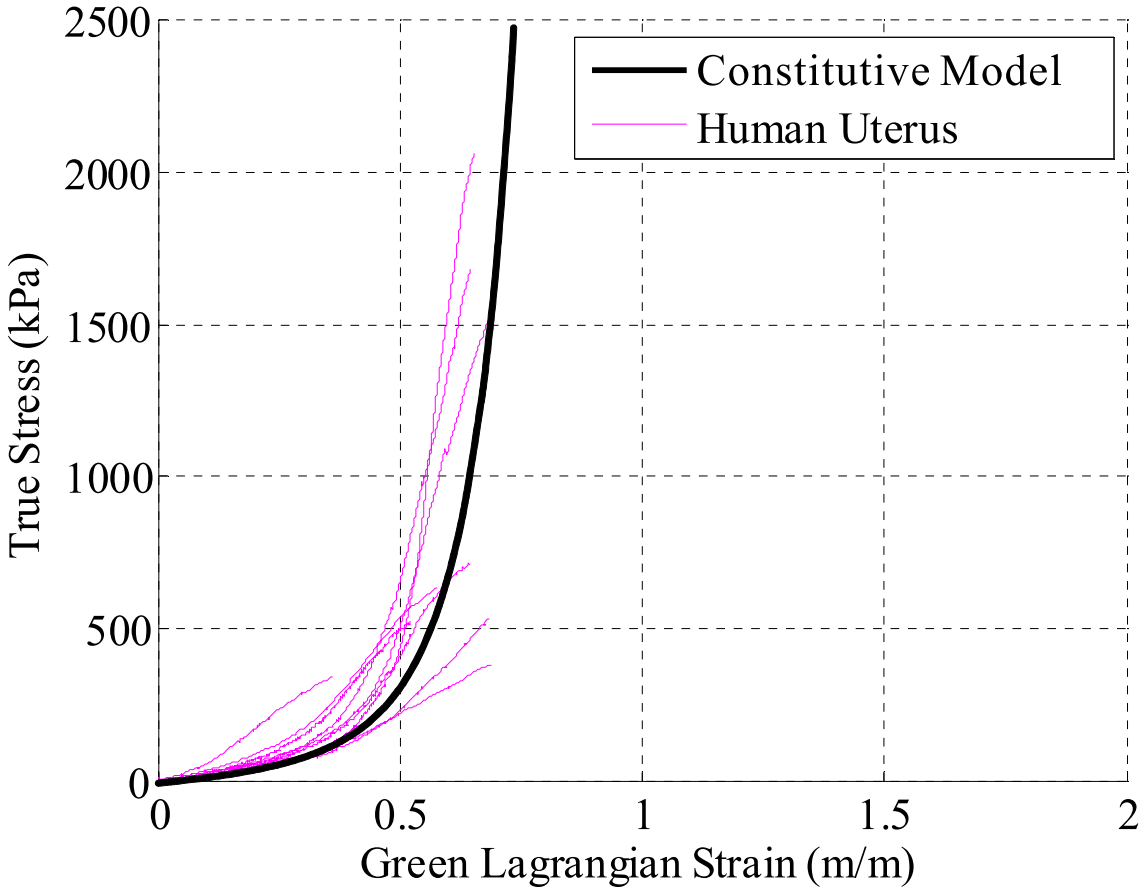

Figure 4.4: Comparison of the results obtained by the numerical simulation of a traction test to the uterine tissue sample and the ones reported by Manoogian. Human uterus values from [Manoogian, 2008].

Chapter 5

Developed Work

5.1 Geometrical and Finite Element Models

5.1.1 Foetal Model

The foetal finite element model, shown in Fig. 5.1, is composed by 48148 tetrahedral (ABAQUS C3D4H type) finite elements and is the model used by Parente [Parente, 2008]. Its position is appropriate for delivery, with both arms and legs leaning against the trunk. The dimensions of the foetus are concordant with the literature dimensions for a full-time foetus [Llewellyn-Jones, 2004].

In order to control the movement of the foetus, 4 groups of elements were given the properties of rigid elements and a reference point was assigned to each group (Fig. 5.2). Controlling the displacements and rotations of these 4 reference nodes, is possible to define the movement of the foetus.

Excluding these 4 groups, the remaining foetal finite elements were given the material properties of a high stiffness material (hyper-elastic Neo-Hookean constitutive model, $C_{10} = 80000$ MPa and $D_1 = 1.0^{-6}$). Thus, in comparison with the uterus, the foetus can be considered a rigid body, reducing its deformations. As the main goal of this work is to study the biomechanics of the uterus, this approach facilitates the convergence of the numerical simulation, maintaining the uterine properties.

5.1.2 Uterine Model

The uterine geometrical model is composed by 7263 hexahedral (ABAQUS C3D8H type) finite elements. It represents only the middle layer of the uterus, the myometrium, because it is the only contractile layer. The top layer, the perimetrium, is a thin layer of connective tissue connected to the broad ligament and the endometrium is a mucous layer with more importance in the early stages of implantation of the ovum, and therefore were not considered in this model.

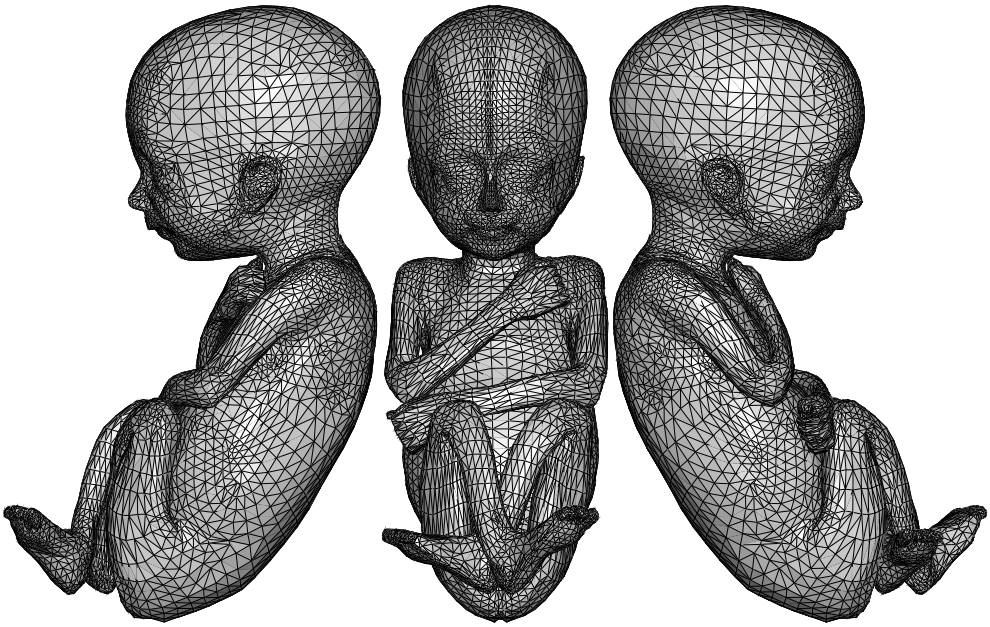

(a) Right view (b) Front view (c) Left view

Figure 5.1: Details of the foetus finite element model.

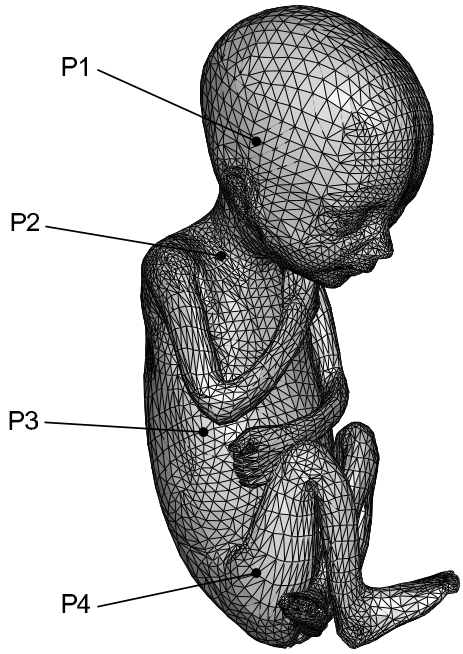

Figure 5.2: Foetal model and points used to control its movements.

5.1.2.1 Uterus Design

The internal uterine surface was designed in a CAD software (Fig. 5.3) through several circles created around the foetal model. As it was designed based on the foetus, its dimension can be considered anatomically correct, since there are no literature values for term-pregnancy uterus size. Afterwards, the surface created was meshed in ABAQUS and extruded in FEMAP software. The model has 3 layers of elements with a total thickness of 10 mm. This value is an approximation of the average thickness of the myometrium (9 mm [Degani et al., 1998]) and was considered in all the model for simplicity's sake. These layers only represent the middle layer of the uterus, the myometrium, since it is the only contractile layer.

The uterus was modelled with complete effacement and dilation (Fig. 5.4), as in the beginning of the second stage of labour.

Figure 5.3: Uterine surface designed in the CAD software.

5.1.2.2 Uterus Adjustment

The design uterine model was very loose, since it was very difficult to design a tight model directly on the CAD software. In order to overcome this problem, a simulation was performed, in which a thermal expansion property was used. In this simulation, the uterine elements were given elastic properties(E=1000 Mpa and

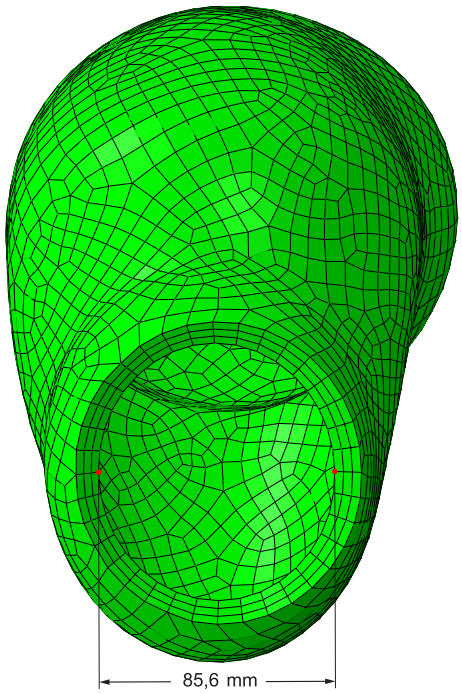

Figure 5.4: Uterine dilation at the beginning of the simulation.

v=0.0), as well as as thermal expansion coefficient (α=-0.2C^{-1}). This has a negative value since the wanted operation was a thermal contraction, instead of a expansion. The result of this test was a tighter uterus, closer to the reality.

5.1.2.3 Myometrial Fibres

The constitutive model used for the uterus needs the definition of the muscular fibres direction, for each finite element. In order to obtain these directions, a simple simulation was performed, where the uterus was considered to be an elastic material (E=10 MPa, v=0.3). To this model, an pressure was applied in the internal surface, causing the deformation seen on Fig. 5.6.

By Murray [Murray et al., 2006], the different directions (radial and longitudinal) of the fibres on three myometrial layers are known. Thus, it was assumed, in the later uterine models, that for each finite element, the muscular fibre direction was coincident with the maximum or the middle principal stress direction (Fig. 5.7), for the radial and longitudinal fibres, respectively.

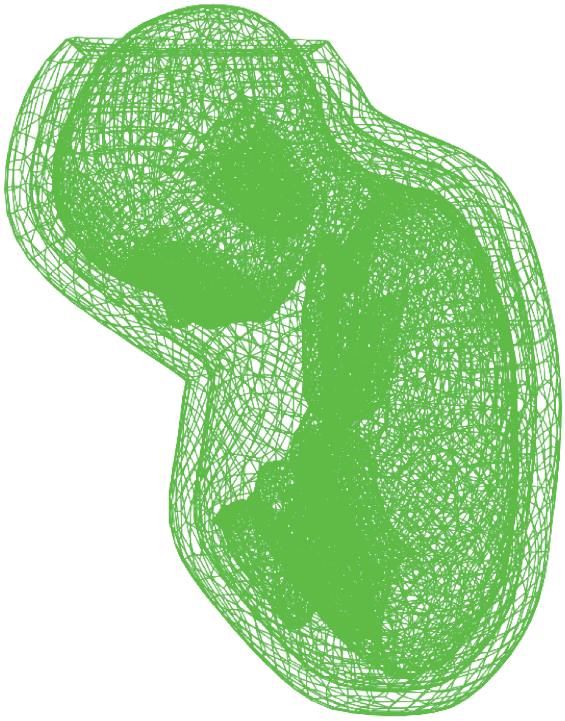

(a) Model before the thermal contraction simulation.

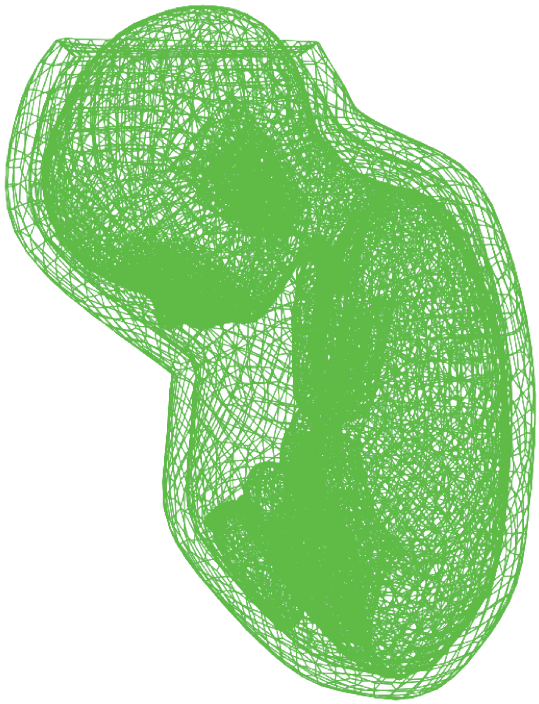

(b) Deformed model after the thermal contraction.

Figure 5.5: Thermal contraction of the uterine model.

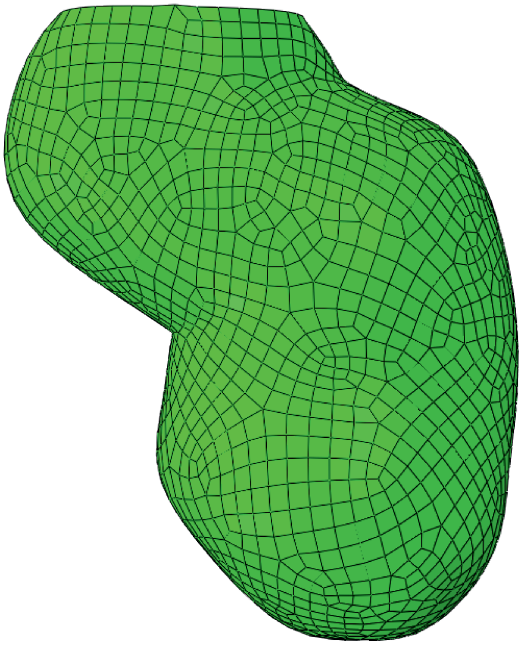

(a) Model before the application of the internal pressure.

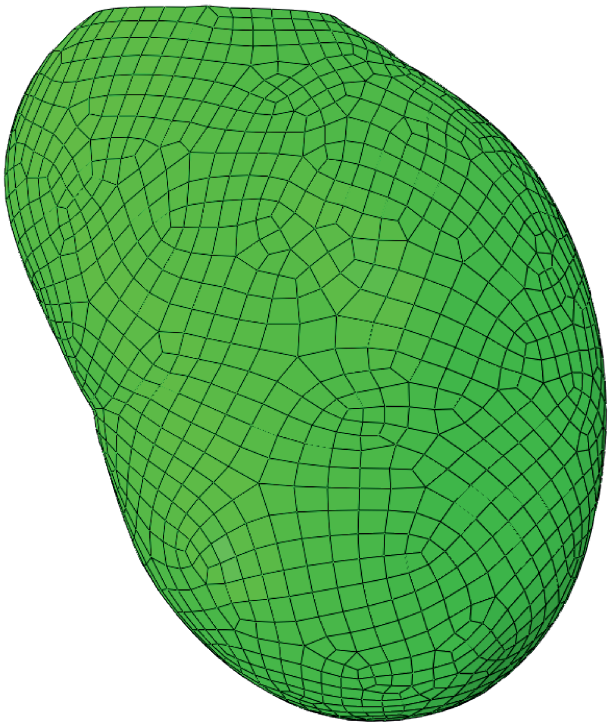

(b) Deformed model after the application of the pressure.

Figure 5.6: Deformation of the uterine model, for the attainment of the muscular fibres directions.

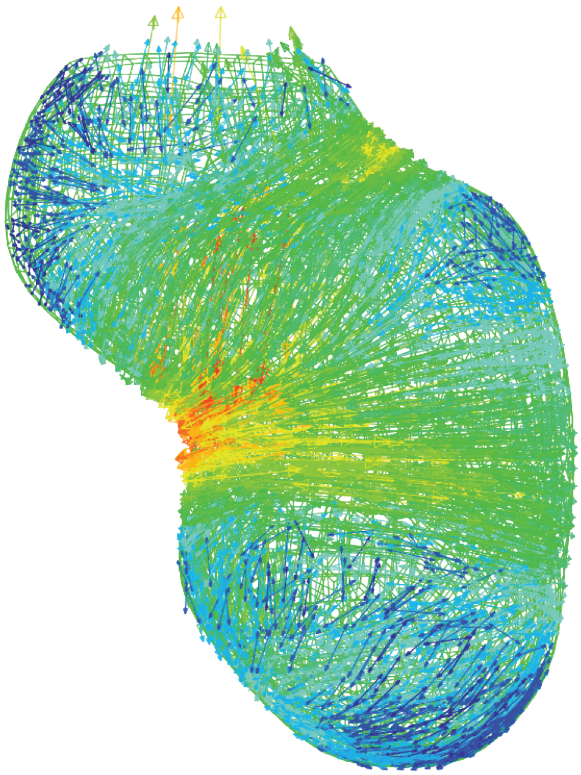

(a) Maximum Principal Stress direction obtained.

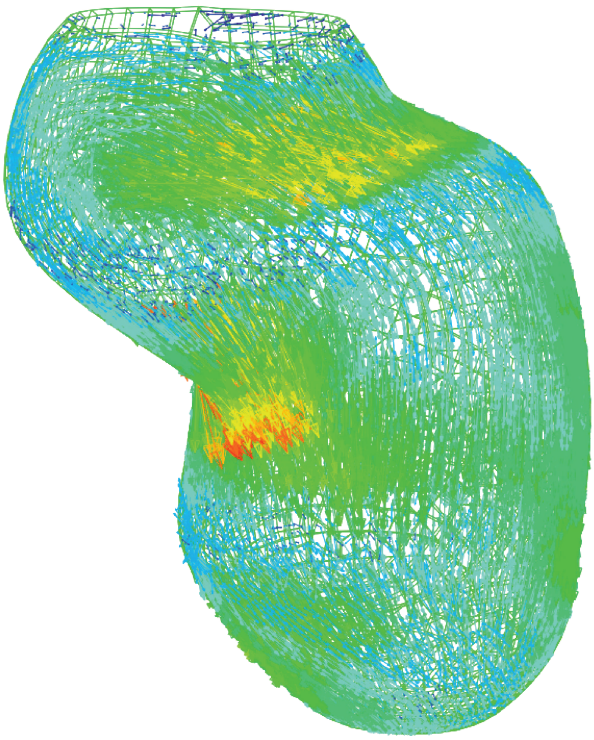

(b) Middle Principal Stress direction obtained.

Figure 5.7: Directions obtained for the muscular fibres.

5.1.3 Maternal Pelvic Bones

A simplified model of the pubic symphisis was also designed (Fig. 5.8). It was designed as a rigid discrete surface, and was only included in the simulation without imposed trajectory. Its inclusion was due to the necessity of assistance for the extension of the foetal head.

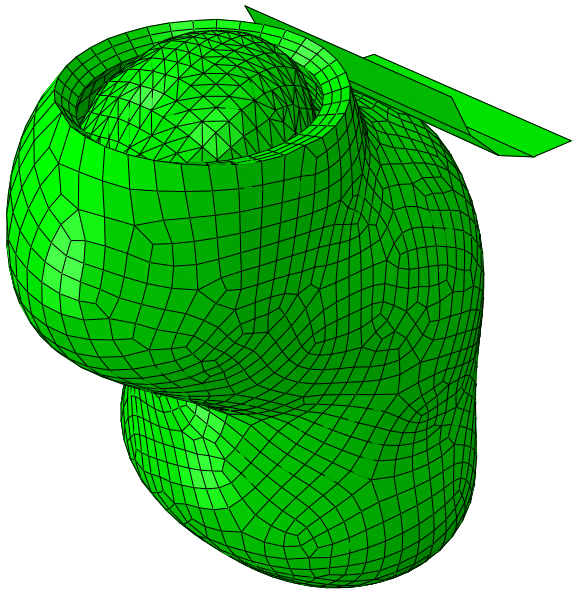

Figure 5.8: Design and position of the pubic symphisis simplified model.

5.2 Numerical Simulations of Delivery

Labour is a sequence of uterine contractions that results in effacement and dilatation of the cervix and voluntary bearing-down efforts leading to the expulsion of the foetus through the vagina. In order for the delivery to occur, the foetus must undergo several movements, known as the mechanics of labour.

The mechanism of labour in vertex position consists of the following cardinal movements: engagement of the presenting part, descent of foetal head below the pelvic inlet and of the presenting part through the birth canal, flexion and rotation of the foetal head to present the smallest possible diameter of the foetal head to the maternal pelvis, extension, external rotation of the foetal head after delivery and finally, expulsion.

The vertex position is when the baby's head is positioned to come out first, before the rest of the body, at birth. During normal labour the baby's head rotates

so that the baby's face is toward the mother's back and the top of the baby's head is facing up, the occipito-anterior position.

All the finite element simulations were made with a non-linear analysis using the implicit version of the ABAQUS software.

The finite element simulations presented in the following sections were made with different approaches. In the first one, the foetal model's translations and rotations are not restricted, and its movements are a consequence of the uterine contractions and external pressures. In the second simulation, a foetal trajectory was imposed, in order to obtain the stresses and strains on the uterus.

To our knowledge, this simulation is the first one using realistic foetal and uterine models.

In this work, the second stage of labour was simulated. In this stage, the uterus is already completely dilated and the cervix effaced. The foetus was moved in order to be in the correct position for a simulation of a delivery in the vertex presentation and occipito-anterior position.

5.2.1 Without Imposed Foetal Trajectory

In this approach, the goal was to deliver the foetus only by uterine muscle contractions and external pressures, simulating the maternal pushes. The pubic symphysis surface created was included in this simulation, in order to help the foetus head extension.

Fig. 5.9 shows the different uterine segments that were subject to contraction.

In Fig. 5.10, the surfaces where the pressures are applied are shown. These surfaces were also chosen in order to facilitate the extension of the foetal head.

In Fig. 5.11, the simulation progression algorithm is shown.

5.2.2 With Imposed Foetal Trajectory

In this approach, some of the cardinal movements were simulated. Since the simulation started on the beginning of the second stage of labour, expulsion was not simulated and the foetus was already positioned after some cardinal movements, the movements simulated were the extension of the foetal head and several displacements of the head and body of the foetus.

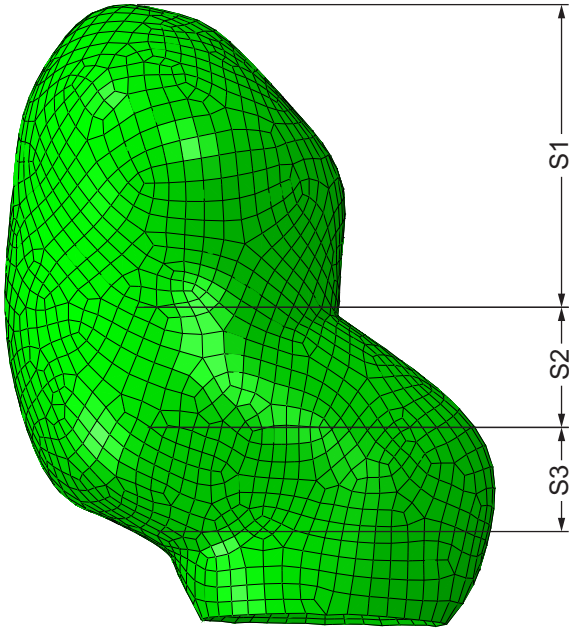

Figure 5.9: The different contractile uterine segments created.

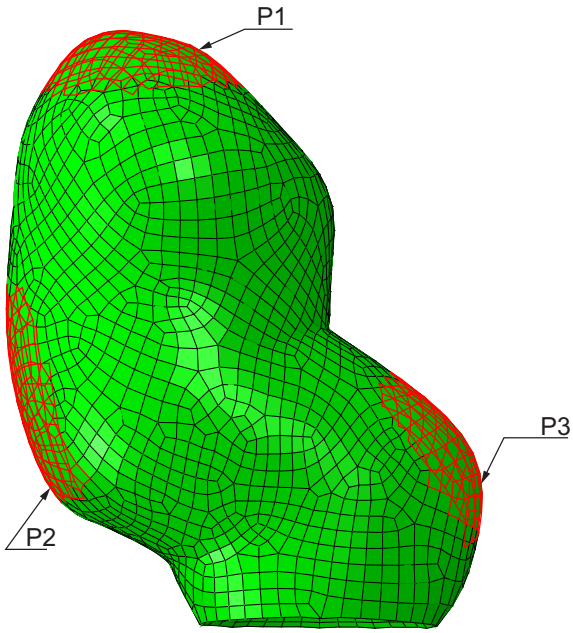

Figure 5.10: Uterine surfaces subject to application of external pressures.

Step	Simulation
Step 1	Pressure applied on P1
Step 2	Contraction of S1 and pressure on P1
Step 3	Pressure on P1
Step 4	Contraction of S1
Step 5	Pressure on P2 and P3
Step 6	Contraction of S2 and S3
Step 7	Contraction of S3

Figure 5.11: Algorithm for the simulation without imposed trajectory.

Chapter 6

Results

6.1 Simulation Without Foetal Imposed Trajectory

The results of the simulation without foetal imposed trajectory is shown on Fig. 6.1. As can be seen, the delivery of the foetus was not completely simulated. The main factors that hindered the good progress of this simulation were the instability of the foetal model, whose movements were not restricted, and its complexity, which caused problems in the contact between the foetus and the uterus. Because of these aspects, the applied uterine contractions and the external pressures could not present the values that occur in reality (approximately 0.003 MPa applied vs 0.4 MPa that occur in a normal labour [Buhimschi et al., 2004]) and did not cause enough stress that could push the foetus downward and complete the delivery.

6.2 Simulation With Foetal Imposed Trajectory

The position of the foetus during the simulation with imposed trajectory is shown on Fig. 6.2. Fig. 6.2a shows the initial position of the foetus, which was positioned presenting the smallest diameter of the head. Fig. 6.2f shows the final position of the foetus, after its displacement and the extension of the head.

In order to evaluate the stresses and strains obtained, several paths along the uterus were defined, as shown in Fig. 6.3. With these paths defined, the stretch ratio can also be calculated and presented. The stretch ratio is defined by the ratio between the current length and the initial length of the path. Measuring the length of the levels during the simulation and knowing their initial value allow us to determine the evolution of the stretch values for each path. The initial lengths for the different levels are also shown on Fig. 6.3.

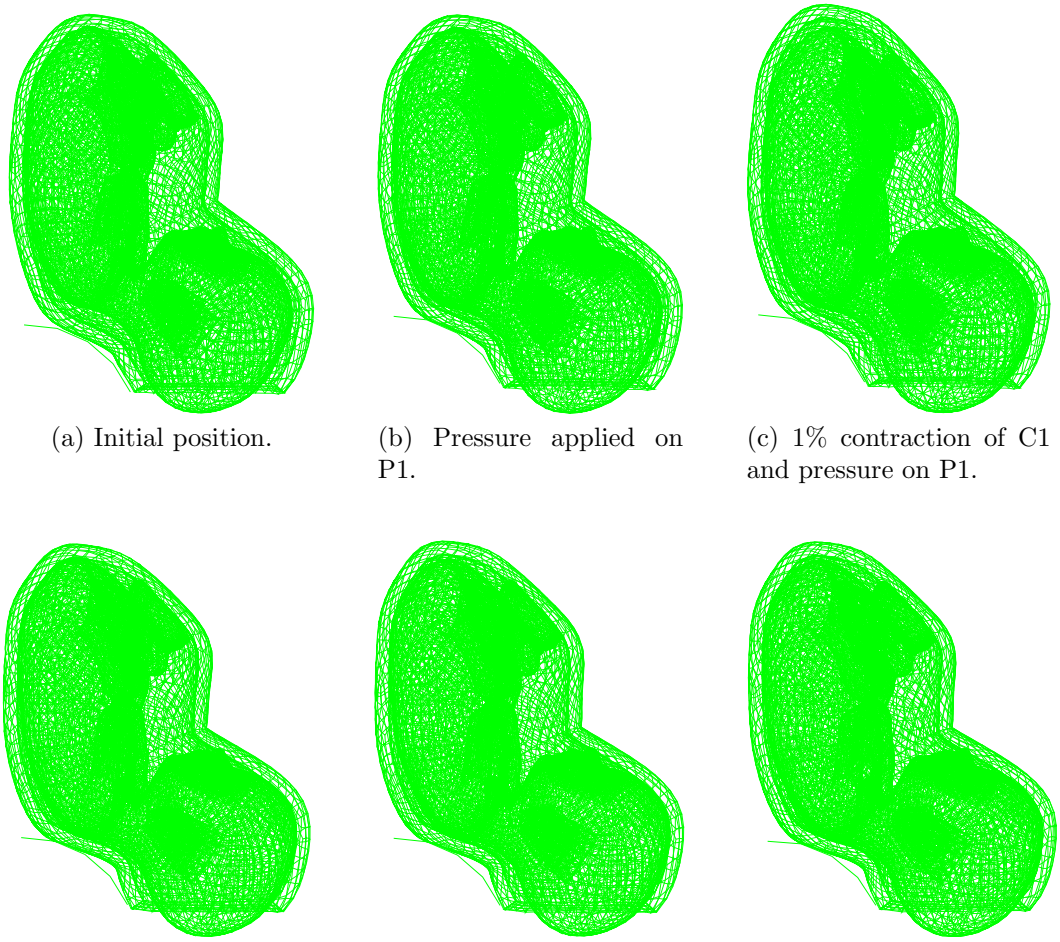

(a) Initial position.

(b) Pressure applied on P1.

(c) 1% contraction of C1 and pressure on P1.

(d) Pressure on P1.

(e) 2% contraction of C1.

(f) Pressure on P2 and P3.

Figure 6.1: Simulation without imposed trajectory.

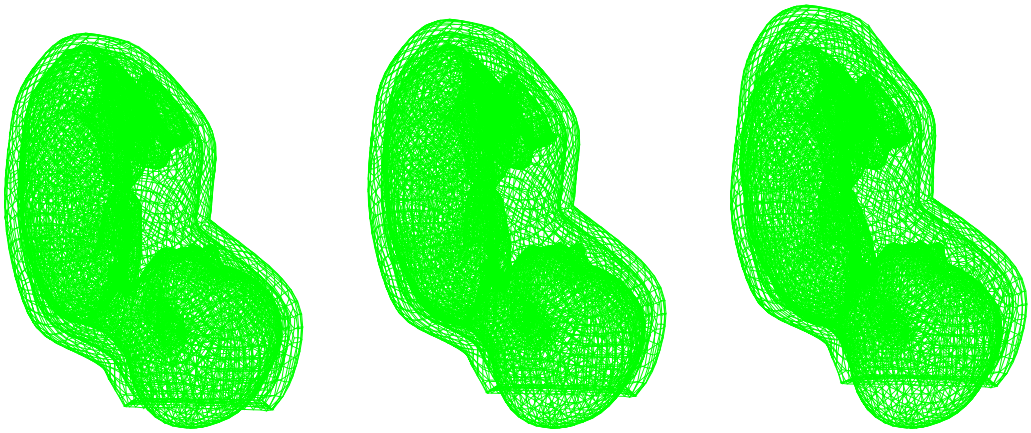

(a) Vertical displacement of 0 mm.

(b) Vertical displacement of 10 mm.

(c) Vertical displacement of 20 mm.

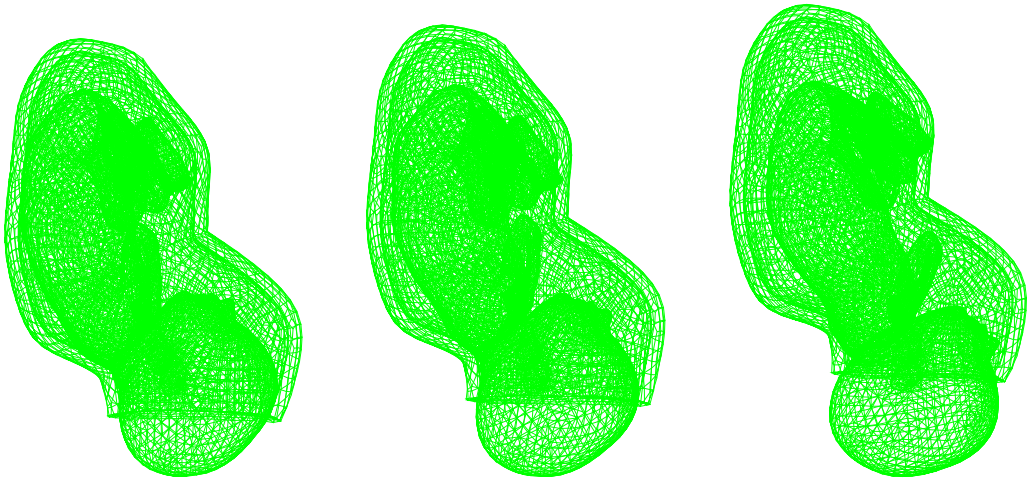

(d) Vertical displacement of 30 mm.

(e) Vertical displacement of 40 mm.

(f) Vertical displacement of 50 mm.

Figure 6.2: Vertical displacement of the foetal head during the simulation with imposed trajectory.

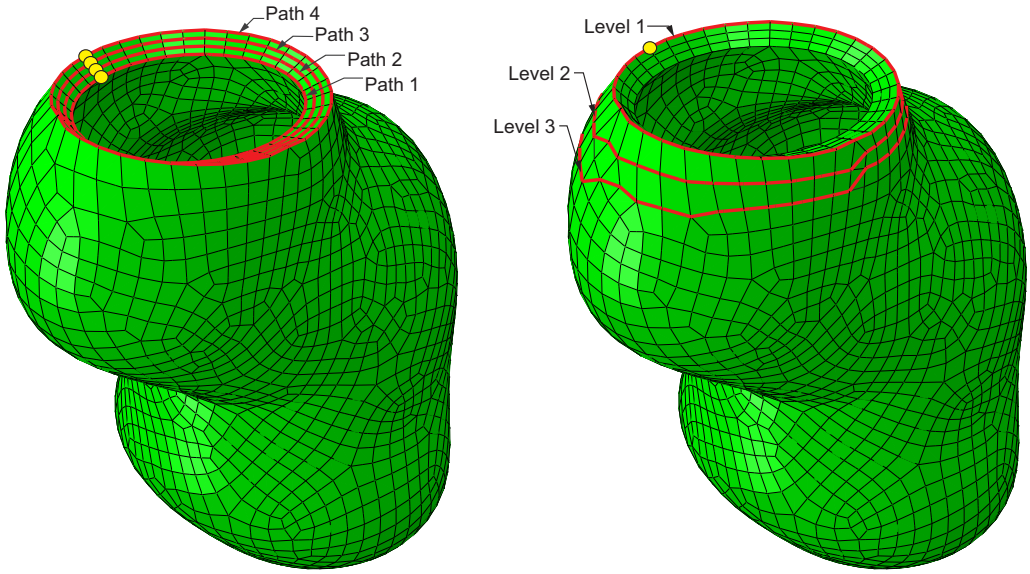

Levels	Initial Length	Length at 50 mm descent
Path 1	27.2 cm	31.3 cm
Path 2	28.9 cm	33.0 cm
Path 3	30.6 cm	34.8 cm
Path 4 / Level 1	32.4 cm	36.6 cm
Level 2	35.6 cm	38.1 cm
Level 3	38.8 cm	40.0 cm

Figure 6.3: Levels and paths used to evaluate the results. The starting points are represented by the yellow circles. Both levels and paths advance in a counterclockwise direction.

The maximum value of stretch was approximately 1.17, and occurred during the extension of the foetal head, on the Path 1 at a vertical displacement of 40mm.

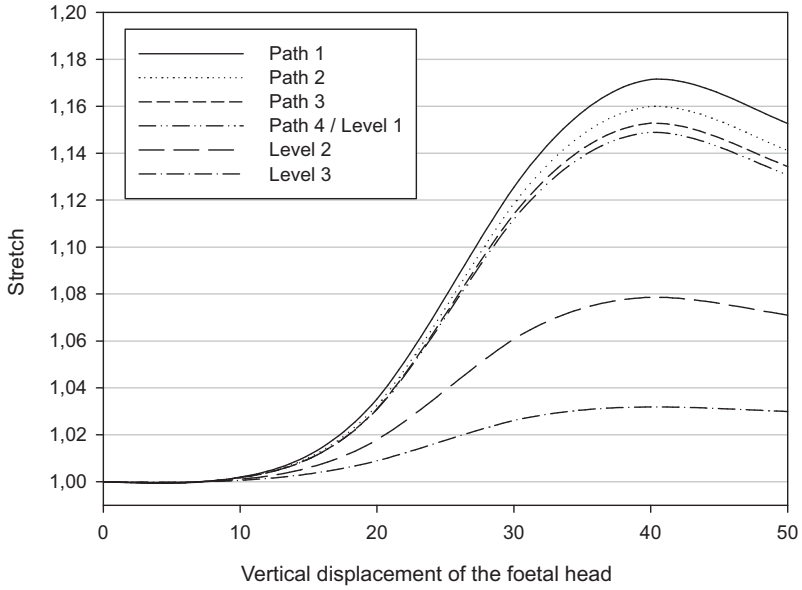

Figure 6.4: Stretch values obtained along the different paths and levels.

The distribution of the maximum principal stresses is shown in Fig 6.5 and it can be observed that the maximum values appear on the most anterior area of the uterus. The maximum value for the maximum principal stress detected was 0.043 MPa, during the extension movement of the head.

Fig. 6.6 and 6.7 show the results obtained for the logarithmic maximum principal strain and the maximum principal stress along the different paths and levels. The maximum principal strain is defined as the ratio between the variation in length and the original tissue length. Then, the logarithmic function is applied to the ratio results. These results were evaluated for a foetal head descent of 20, 30, 40, 45 and 50 mm.

In order to facilitate the comparison of results between the different paths and levels, the normalized length (varies between 0 at the start point and 1 at the end point) was used.

Observing Fig. 6.6, for the different vertical displacements of the foetal head, the maximum value of strain, 0.30, was obtained for a vertical displacement of 45 mm for the Path 1, as can be seen on Fig. 6.6d. At this displacement, the foetal head is almost completely extended.

By using this method, it is possible to evaluate the different levels at each point. Thus, it can be concluded that the region that present higher values of strain is the anterior region of the cervix (0.8 normalized length on Fig. 6.6), which contacts

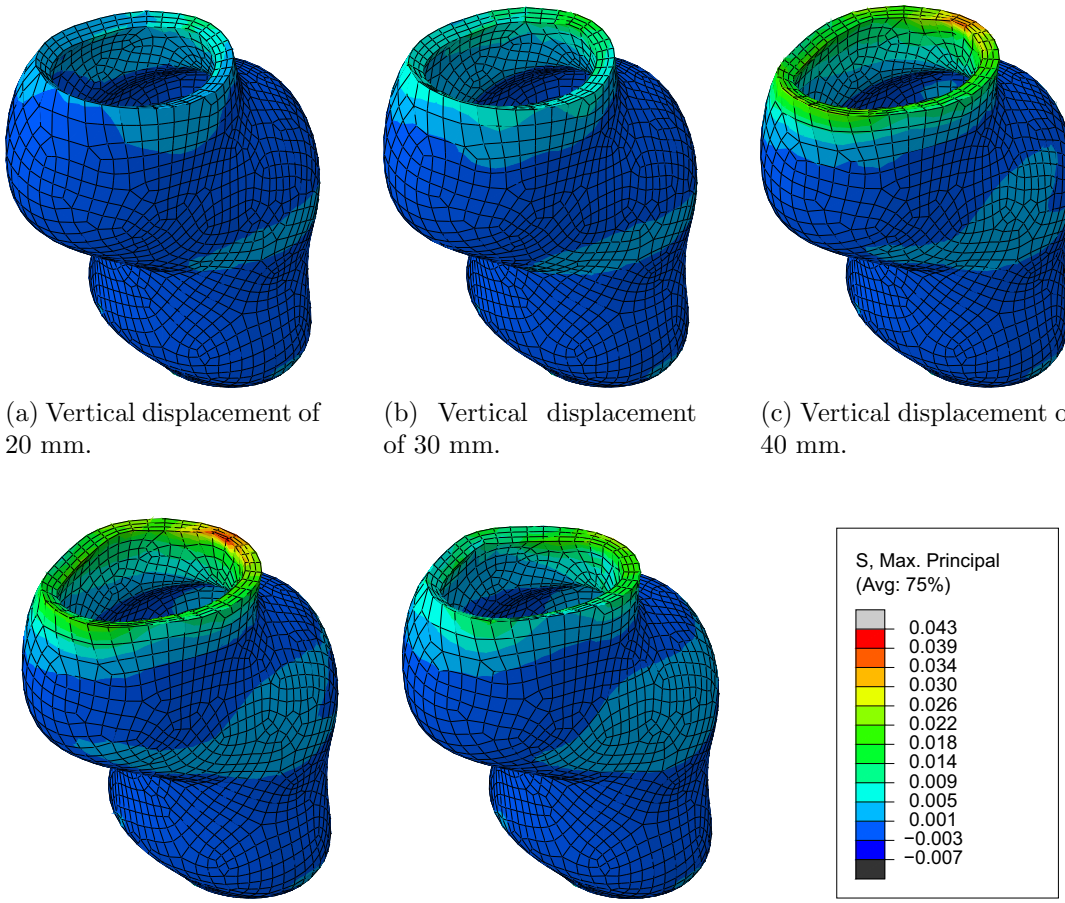

(a) Vertical displacement of 20 mm.

(b) Vertical displacement of 30 mm.

(c) Vertical displacement of 40 mm.

(d) Vertical displacement of 45 mm.

(e) Vertical displacement of 50 mm.

(f) Maximum Principal Stress values.

Figure 6.5: Distribution of the Maximum Principal Stresses (MPa).

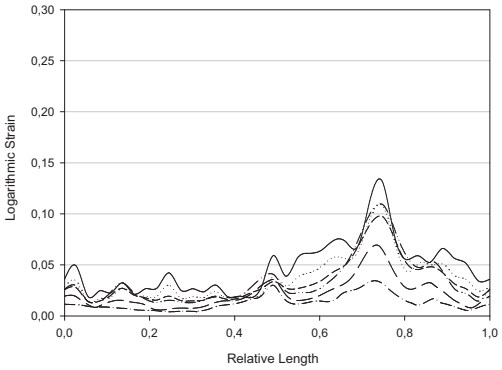

(a) Vertical displacement of 20 mm.

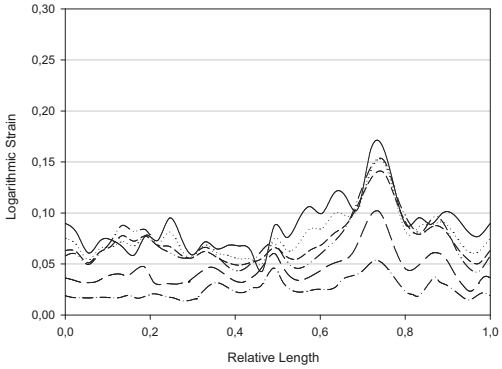

(b) Vertical displacement of 30 mm.

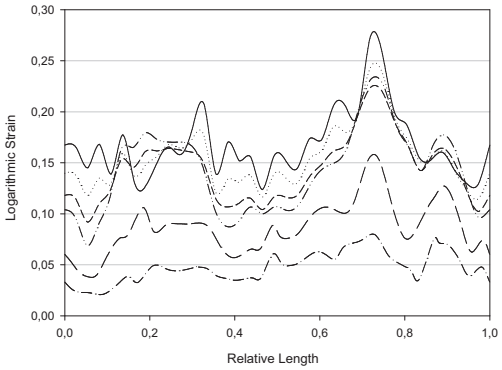

(c) Vertical displacement of 40 mm.

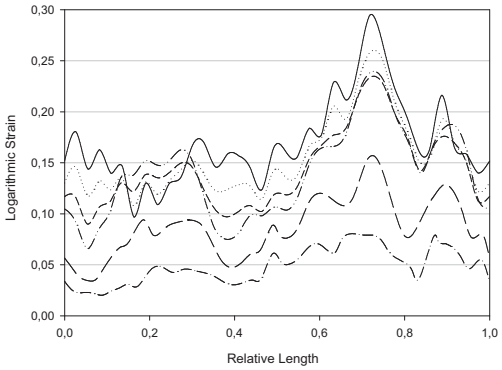

(d) Vertical displacement of 45 mm.

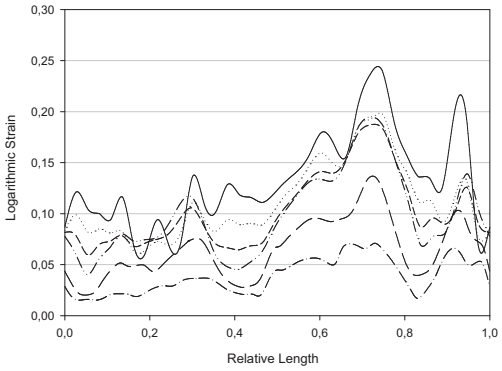

(e) Vertical displacement of 50 mm.

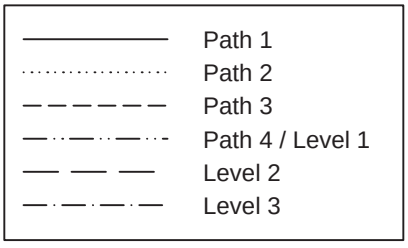

(f) Legend.

Figure 6.6: Logarithmic Maximum Principal Strain along the different paths and levels.

with the foetal head.

The stretch values presented in Fig. 6.4 are more conservative, because of the assumption that the deformation is uniform along the levels.

Fig. 6.7 shows the evolution of the maximum principal stresses along the different paths and levels, for different vertical displacements of the foetal head. The higher values of stress occur, as expected, at the same regions and for the same displacements of the higher strain values. Thus, the maximum stress, 0.043 MPa, occurs in Path 1 at 80% of its length, which is the anterior region of the cervix, as can be seen on Fig. 6.7d.

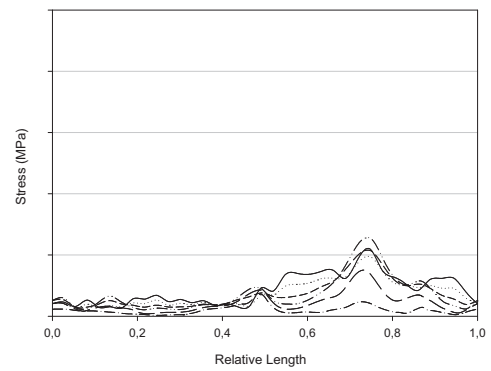

(a) Vertical displacement of 20 mm.

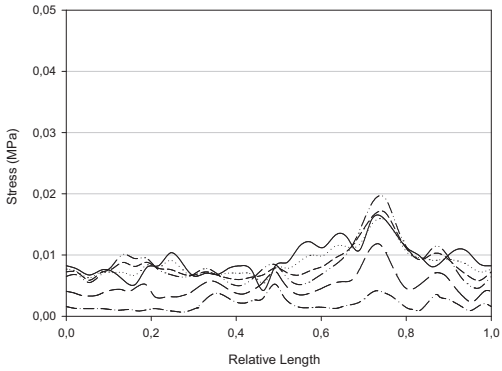

(b) Vertical displacement of 30 mm.

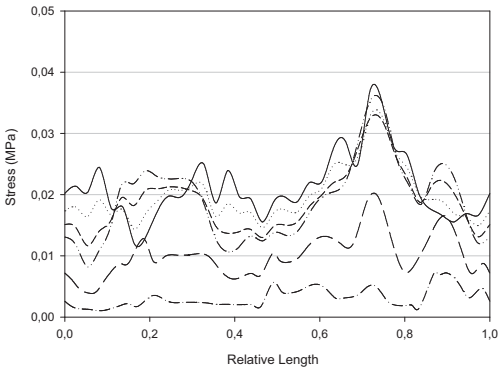

(c) Vertical displacement of 40 mm.

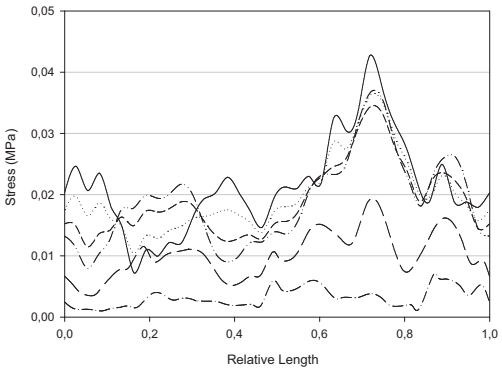

(d) Vertical displacement of 45 mm.

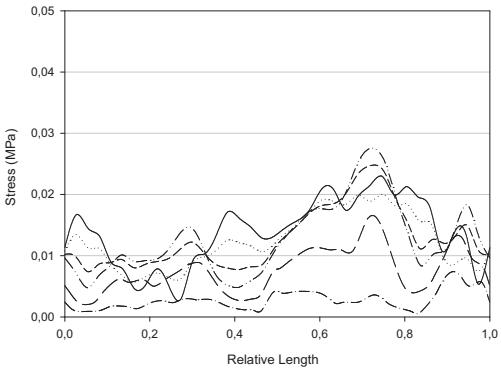

(e) Vertical displacement of 50 mm.

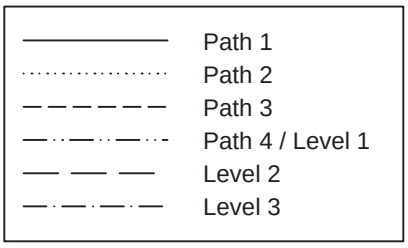

(f) Legend.

Figure 6.7: Maximum Principal Stresses (MPa) along the different paths and levels.

Chapter 7

Conclusions

7.1 Conclusions

In Chapter 6 the simulations conducted in this work were presented. Both simulations presented were for vaginal deliveries in vertex position.

For the first simulation, the one without imposed foetal trajectory, the inclusion of the bony pelvis and remaining pelvic floor tissues will be necessary. Without these, numerical instabilities will occur and the delivery will not complete. Thus, the foetal movements could not be studied, in order to be included in childbirth simulators.

However, the construction of the uterine model including the uterine fibres directions was successfully accomplished, the constitutive parameters were adjusted in accordance with the experimental data and the uterine contractions were also successfully simulated.

Although other simulations including the uterus, without imposed trajectories, were already performed by Buttin [Buttin et al., 2009], this work was the first, to the best of our knowledge, to try to include active muscular uterine contraction in order to drive the foetus and to use a complete realistic foetal model in a vaginal delivery simulation.

Regarding the second simulation conducted, the one with foetal imposed trajectory, the desired cardinal movement of the second stage of labour, the foetal head extension, was successfully performed. The maximum stretch values obtained in this work, approximately 1.17, correspond to the most interior circumference of the cervix (Path 1), during the foetal head extension (vertical displacement of 40mm), when it presents its largest diameter to the uterus. Despite not being a very high value of stretch, we have to take into account that the cervix had already underwent dilation and effacement in the previous stages of labour. Relatively to the logarithmic maximum principal strain values, the maximum value obtained was 0.30, for

a vertical displacement of 45 mm on anterior region of the Path 1. At this displacement, the foetal head is almost completely extended. Regarding the maximum principal stress, the maximum value, 0.043 MPa, occurred, as expected, in the same local and for the same displacements of the higher strain values, i.e. the anterior region of the cervix.

There are not other works, as far as we know, that studied the stresses and strains obtained at the uterus during vaginal delivery, and consequently, no comparisons can be performed.

7.2 Future Work

This thesis presented a finite element model capable of a childbirth simulation, with the foetus in the vertex presentation. There are, although, many aspects that could affect the final results and could be included in order to perform a better simulation of this event, allowing it to become a helpful tool for obstetricians. For that to happen, it is necessary to this model to be adjusted to each case of pregnancy, which needs the creation of custom geometrical models, through information obtained, for example, by Magnetic Resonance Imaging (MRI). The inclusion of the bony pelvis and the remaining pelvic floor tissues, as stated before, is of great importance too.

The characterization of the mechanical properties of the pregnant uterine tissue is also an aspect that needs more study, since the material properties used in this work correspond to a non-pregnant uterus. Also, the inclusion of a damage model on the uterine constitutive model could be an important improvement. Another significant feature that could be implemented in the model is the foetal head moulding. Also, numerical simulations of assisted delivery (forceps and Kiwi ventouse) could be performed.

In the future, with the inclusion of some oh these improvements, this model could simulate realistically a vaginal delivery, as well its effects on the uterine tissue and provide data for childbirth simulators, becoming a valuable tool for obstetricians.

Bibliography

D Aulignac, J A C Martins, E B Pires, T Mascarenhas, and R M Natal Jorge. A shell finite element model of the pelvic floor muscles . *Computer Methods in Biomechanics and Biomedical Engineering*, 8(5):339–347, October 2005.

L F Bastos, M F Lobo, W van Meurs, and D Ayres-de Campos. An intrauterine pressure generator for educational simulation of labour and delivery . *Medical Engineering & Physics*, 32(7):740–745, September 2010.

L F Bastos, W van Meurs, and D Ayres-de Campos. A model for educational simulation of the evolution of uterine contractions during labor. *Computer Methods and Programs in Biomedicine*, 107(2):242–247, August 2012.

C S Buhimschi, I A Buhimischi, A M Malinow, and C P Weiner. Intrauterine Pressure during the second stage of labor in obese women. *Obstetrics & Gynecology*, 103(2):225–230, 2004.

R Buttin, F Zara, B Shariat, T Redarce, and G Grange. Biomechanical Simulation of the Fetal descent without Imposed Theoretical Trajectory . pages 5263–5266, 2009.

B Calvo, E Peña, P Martins, T Mascarenhas, M Doblaré, R M Natal Jorge, and A Ferreira. On modelling damage process in vaginal tissue . *Journal of Biomechanics*, 42(5):642–651, March 2009.

L Chen, J A Ashton-Miller, and J O L DeLancey. A 3D finite element model of anterior vaginal wall support to evaluate mechanisms underlying cystocele formation. *Journal of Biomechanics*, 42(10):1371–1377, July 2009.

S Degani, Z Leibovitz, I Shapiro, R Gonen, and G Ohel. Myometrial Thickness in Pregnancy: Longitudinal Sonographic Study. *Journal of Ultrasound in Medicine*, 17:661–665, 1998.

O Dupuis, R Silveira, and T Redarce. Operative vaginal delivery rate and neonatal associated complications in 2002 in the"Aurore"hospital network. *Gynecology Obstetrique & Fertilite*, 2003.

O Eytan and D Elad. Analysis of intra-uterine fluid motion induced by uterine contractions . *Bulletin of Mathematical Biology*, 61(2):221–238, March 1999.

S G Gabbe, J R Niebyl, and J L Simpson. *Obstetrics: Normal and Problem Pregnancies*. Elsevier, 5th ed edition, 2007.

J E Hall. *Guyton and Hall Textbook of Medical Physiology*. 2010.

M L R Harkness and R D Harkness. Changes in the physical properties of the uterine cervix of the rat during pregnancy. *The Journal of Physiology*, 1959.

M L R Harkness and R D Harkness. The mechanical properties of the uterine cervix of the rat during involution after parturition. *The Journal of Physiology*, 1961.

J D Humphrey and F C P Yin. On constitutive relations and finite deformations of passive cardiac tissue: A pseudostrain-energy function. *Journal of Biomechanical Engineering*, 109(4):298–304, 1987.

H Izumi. Changes in the mechanical properties of the longitudinal and circular muscle tissues of the rat myometrium during gestation. *British Journal of Pharmacology*, 86(1):247–257, July 2012.

S Janda, F C T van der Helm, and S B de Blok. Measuring morphological parameters of the pelvic floor for finite element modelling purposes . *Journal of Biomechanics*, 36(6):749–757, June 2003.

D Jing. Experimental and Theoretical Biomechanical Analyses of the Second Stage of Labor . 2010.

R J A Lapeer. A biomechanical model of foetal head moulding . 1999.

R J A Lapeer and R W Prager. Fetal head moulding: finite element analysis of a fetal skull subjected to uterine pressures during the first stage of labour . *Journal of Biomechanics*, 34(9):1125–1133, September 2001.

S-L Lee, A Darzi, and G-Z Yang. Subject specific finite element modelling of the levator ani . *Medical image computing and computer-assisted intervention : MICCAI International Conference on Medical Image Computing and Computer-Assisted Intervention*, 8(Pt 1):360–367, 2005.

S-L Lee, E Tan, V Khullar, W Gedroyc, A Darzi, and G-Z Yang. Physical-based statistical shape modeling of the levator ani . *IEEE Transactions on Medical Imaging*, 28(6):926–936, June 2009.

X Li, J A Kruger, J-H Chung, M P Nash, and P M F Nielsen. Modelling childbirth: comparing athlete and non-athlete pelvic floor mechanics . *Medical image computing and computer-assisted intervention : MICCAI International Conference on Medical Image Computing and Computer-Assisted Intervention*, 11(Pt 2): 750–757, 2008.

Z Li, J E Alonso, J-E Kim, J S Davidson, B S Etheridge, and A W Eberhardt. Three-dimensional finite element models of the human pubic symphysis with viscohyperelastic soft tissues . *Annals of Biomedical Engineering*, 34(9):1452–1462, September 2006.

Z Li, J-E Kim, J S Davidson, B S Etheridge, J E Alonso, and A W Eberhardt. Biomechanical response of the pubic symphysis in lateral pelvic impacts: a finite element study . *Journal of Biomechanics*, 40(12):2758–2766, 2007.

K-C Lien, B Mooney, J O L DeLancey, and J A Ashton-Miller. Levator ani muscle stretch induced by simulated vaginal birth . *Obstetrics & Gynecology*, 103(1): 31–40, January 2004.

D Llewellyn-Jones. *Fundamentals of Obstetrics and Gynaecology*. Elsevier Health Sciences, 2004.

C D Maggio, S R Jennings, J L Robichaux, P C Stapor, and J M Hyman. A modified Hai-Murphy model of uterine smooth muscle contraction . *Bulletin of Mathematical Biology*, 74(1):143–158, January 2012.

S J Manoogian. Protecting the Pregnant Occupant: Dynamic Material Properties of Uterus and Placenta. 2008.

S J Manoogian, J A Bisplinghoff, A R Kemper, and S M Duma. Dynamic material properties of the pregnant human uterus. *Journal of Biomechanics*, 45(9):1724–1727, June 2012.

J A C Martins, E B Pires, R Salvado, and P B Dinis. A numerical model of passive and active behaviour of skeletal muscles. *Computer methods in applied mechanics and engineering*, 151(3–4):419–433, 1998.

J A C Martins, M P M Pato, E B Pires, R M Natal Jorge, M P L Parente, and T Mascarenhas. Finite Element Studies of the Deformation of the Pelvic Floor. *Annals of the New York Academy of Sciences*, 1101(1):316–334, February 2007.

H Maul, W L Maner, G R Saade, and R E Garfield. The physiology of uterine contractions. *Clinics in Perinatology*, 30(4):665–676, 2003.

E Mazza, A Nava, M Bauer, R Winter, M Bajka, and G A Holzapfel. Mechanical properties of the human uterine cervix: An in vivo study. *Medical Image Analysis*, 10(2):125–136, April 2006.

J Mizrahi, Z Karni, and W Z Polishuk. Isotropy and anisotropy of uterine muscle during labor contraction . *Journal of Biomechanics*, 13(3):211–218, 1980.

S S Murray, E S McKinney, and T Gorrie. Foundations of Maternal-Newborn Nursing. 2006.

K M Myers, A P Paskaleva, M House, and S Socrate. ScienceDirect com - Acta Biomaterialia - Mechanical and biochemical properties of human cervical tissue. *Acta Biomaterialia*, 2008.

P Niederer, S Weiss, R Caduff, M Bajka, G Szekély, and M Harders. Uterus models for use in virtual reality hysteroscopy simulators. *European Journal of Obstetrics & Gynecology and Reproductive Biology*, 144:S90–S95, May 2009.

K F Noakes, I P Bissett, A J Pullan, and L K Cheng. Anatomically based computational models of the male and female pelvic floor and anal canal . *Conference proceedings: Annual International Conference of the IEEE Engineering in Medicine and Biology Society IEEE Engineering in Medicine and Biology Society Conference*, 1:3815–3818, 2006.

K F Noakes, I P Bissett, A J Pullan, and L K Cheng. Anatomically Realistic Three-Dimensional Meshes of the Pelvic Floor & Anal Canal for Finite Element Analysis. *Annals of Biomedical Engineering*, 36(6):1060–1071, March 2008a.

K F Noakes, A J Pullan, I P Bissett, and L K Cheng. Subject specific finite elasticity simulations of the pelvic floor . *Journal of Biomechanics*, 41(14):3060–3065, October 2008b.

M P L Parente. *Biomechanics of the pelvic floor during vaginal delivery.* PhD thesis, 2008.

M P L Parente, R M Natal Jorge, T Mascarenhas, A A Fernandes, and J A C Martins. Deformation of the pelvic floor muscles during a vaginal delivery . *International Urogynecology Journal and Pelvic Floor Dysfunction*, 19(1):65–71, January 2008.

M P L Parente, R M Natal Jorge, T Mascarenhas, A A Fernandes, and J A C Martins. The influence of the material properties on the biomechanical behavior of the pelvic floor muscles during vaginal delivery. *Journal of Biomechanics*, 42 (9):1301–1306, June 2009a.

M P L Parente, R M Natal Jorge, T Mascarenhas, A A Fernandes, and J A C Martins. The influence of an occipito-posterior malposition on the biomechanical behavior of the pelvic floor. *European Journal of Obstetrics & Gynecology and Reproductive Biology*, 144:S166–S169, May 2009b.

M P L Parente, R M Natal Jorge, T Mascarenhas, A A Fernandes, and A L Silva-Filho. Computational modeling approach to study the effects of fetal head flexion during vaginal delivery. *American Journal of Obstetrics & Gynecology*, 203(3): 217 e1–217 e6, September 2010.

M P L Parente, M E T Silva, R M Natal Jorge, A A Fernandes, and T Mascarenhas. Study on the Influence of the Fetus Head Molding during Vaginal Delivery on the Biomechanical Behavior of the Pelvic Floor. *Journal of Biomechanics*, 45(S1): S70, July 2012.

H C Parkington. Some properties of the circular myometrium of the sheep throughout pregnancy and during labour . *The Journal of Physiology*, 1985.

D D Rahn, M D Ruff, S A Brown, and H F Tibbals. Biomechanical properties of the vaginal wall: effect of pregnancy, elastic fiber deficiency, and pelvic organ prolapse. *American Journal of Obstetrics and Gynecology*, 2008.

W N Spellacy, S Miller, A Winegar, and P Q Peterson. Macrosomia-maternal characteristics and infant complications . *Obstetrics and Gynecology*, 66(2):158–161, August 1985.

S Standring, H Ellis, and J C Healy. *The Anatomical Basis of Clinical Practice*. Gray's Anatomy. Churchill Livingstone, 40 edition, 2008.

M A M Taverne, C Naaktgeboren, and G C Van der Weyden. Myometrial activity and expulsion of fetuses. *Animal Reproduction Science*, 2(1):117–131, 1979.

C Vauge, B Carbonne, E Papiernik, and F Ferré. A mathematical model of uterine dynamics and its application to human parturition . *Acta Biotheoretica*, 48(2): 95–105, June 2000.

S Weiss, T Jaermann, P Schmid, P Staempfli, P Boesiger, P Niederer, R Caduff, and M Bajka. Three-dimensional fiber architecture of the nonpregnant human uterus determined ex vivo using magnetic resonance diffusion tensor imaging. *The Anatomical Record Part A: Discoveries in Molecular, Cellular, and Evolutionary Biology*, 288A(1):84–90, 2005.

S Weiss, P Niederer, A Nava, R Caduff, and M Bajka. Inverse finite element characterization of the human myometrium derived from uniaxial compression experiments / Von einaxialen Druckversuchen hergeleitete inverse Finite-Elemente-Charakterisierung des menschlichen Myometriums. *Biomedizinische Technik/Biomedical Engineering*, 53(2):52–58, 2008.